Designer functionally graded viscoelastic materials performance tailored to minimize probabilistic failures in panels subjected to aerodynamic noise

(Received: August 12, 2010. Revised: January 11, 2011. Accepted: July 16, 2012)

Harry H. Hilton[1]
Daniel Hank Lee[1]

Abstract
Dynamic responses of plates with temperature dependent and nonhomogeneous linear viscoelastic functionally graded materials (VFGM) are investigated under lift and aerodynamic noise loadings, and thermal stresses and moments. Due to the strong temperature dependence of viscoelastic properties, thermal gradients in essence produce VFGM in addition to other sources. In a fundamental sense VFGM, as well as their elastic counterparts (EFGM), are non-homogeneous isotropic or anisotropic materials and need to be treated as such. Creep buckling and flutter instabilities, and probabilities of material failures are analyzed to determine plate survival times. Optimum designer materials using inherent viscoelastic damping properties, particularly viscoelastic functionally graded ones, are studied to minimize thermal stress and bending load effects while concurrently lowering failure probabilities and extending survival times. Instead of using “off the shelf” materials for specific service demands, the inverse protocol in essence, leads to discoveries of best material properties and their optimal distributions throughout the structure and its components. Subsequent tasks of how to manufacture such designer materials are not covered here and are left to a separate study.

Keywords: aerodynamic/acoustic dynamic creep buckling, designer viscoelastic materials, functionally graded materials, panel flutter, probabilistic failures, survival times, thermal stresses, viscoelasticity

1. Introduction

Viscoelastic materials are known for their ability to dissipate energy [1 – 3]. This property has been successfully used by the senior author and his colleagues to produce effective passive structural control for column and plate creep buckling, various vibratory modes, and aero-viscoelastic phenomena, such as torsional divergence, and wing and panel flutter. In self-excited systems the application of increased dissipation may stabilize or destabilize such systems depending on the of damping on phase relations.

A comprehensive literature review and analysis of FGMs may be found in [4]. Elastic optimized structures are analyzed in [5 – 18], while a few examples of viscoelastic designer material analyses are presented in [19 – 27].

The general theory of designer viscoelastic materials whose properties are optimized and tailored/engineered as inverse problems to perform specified service task has been developed in [19]. It has been further previously established [20] that in homogeneous viscoelastic materials the shape of the relaxation curve is a major contributor to the material's response performance. In particular, it has been shown that Region $\mathcal{C}$ and and the ratio $\dfrac{E_0}{E_\infty}$ of the relaxation modulus (Regions $\mathcal{A}$ and $\mathcal{E}$) as seen in Fig. 1 are the most influential in dictating material

[1] University of Illinois at Urbana-Champaign (UIUC)
104 South Wright Street, 316 Talbot Lab., Urbana, IL 61801-2935 USA

doi:10.3293/asdj.2012.9

LIST OF SYMBOLS

$a_{ij},\ b_{ijkl}$	relaxation modulus coefficients
A_k^*	aerodynamic coefficients
$\boldsymbol{A}_m$	coefficients of PDEs and IPDEs
BC	boundary condition
c_{VD}	viscous mechanical dampping coefficient
$C^*_{ijkl}\quad C_{ijkl}$	compliances
$C^*_{ijkln}\quad C_{ijkln}$	compliance coefficients
$D^*\quad D$	bending stiffnesses
$D^*_{ijkln}\quad D_{ijkl}$	bending stiffness coefficients
$E^*_{ijkl}\quad E_{ijkl}$	relaxation moduli
$E_{ijkl0}\quad E_0$	elastic Young's modulus
$E^*_{ijkln}\quad E_{ijkln}$	relaxation moduli coefficients
E_{SD}	structural damping coefficient
F_A	aerodynamic force (lift)
$\mathcal{F}(x,t)$	functionally graded material distribution
FGM, EFGM, VFGM	functionally graded material, elastic & viscoelastic
g, g_w, g_θ	structural damping coefficient
IPDE	integral partial differential equation
N	summation limit in modulus, compliance Prony series
N_{ijkl}	in-plane force
$\boldsymbol{P}, \boldsymbol{Q}$	viscoelastic differential operators
PDE	partial differential equation
$S_m,\ \boldsymbol{S}$	parameters to be optimized
t	time
T	temperature
$\boldsymbol{u}$	generalized displacement
V	free stream air velocity
V_f	flutter velocity
V_{ult}	maximum velocity causing material structural failures
w	bending deflection
$\boldsymbol{x}\{x_1, x_2, x_3\}$	Cartesian coordinates
$x,\ y,\ z$	Cartesian coordinates
α_r	rigid body angle of attack
Δp_{CP}	cabin pressure
ϵ_{kl}	strain components
ρ	free stream air density
σ_{kl}	stress components
τ_{klmn}	relaxation time

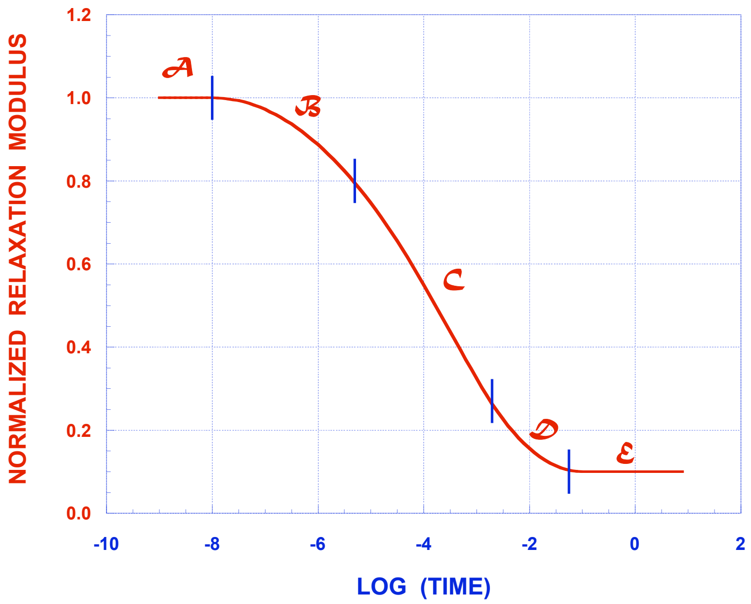

Figure 1: Relaxation modulus regions

dissipation rates. Consequently, such relaxation modulus functions are tailored through optimization of appropriate functionally graded viscoelastic materials to produce the desired designer material performance. In case of composites, for instance, this tantamount to tailoring stacking sequences, fiber orientation, number of plies, properties of fibers and matrices, etc. Relaxation moduli are, of course, highly temperature sensitive and performances are evaluated relative to thermal operational demands.

Functionally graded elastic (EFGM) or viscoelastic (VFGM) materials are essentially and fundamentally nonhomogeneous and anisotropic materials where the spatial and/or temporal material variations are prescribed by specific manufacturing protocols [25] or imposed through service temperature distributions. These predetermined nonhomogeneous and anisotropic material property variations can be realized, for instance, by prescribing *a priori* deterministic or random spatial changes in size, number, orientation, or materials of fibers in composites during manufacture. Inclusion of nano materials in controlled quantities into a polymer or metal matrix is another example of a composite VFGM. Other examples such as use of successful irradiation techniques to produce nonhomogeneous EFGM are described in [28 – 32]. Additionally, viscoelastic material properties can be strongly influenced in service by proper temperature control and thusly comprise another form of FGM.

Passive control of static or dynamic deflections, stresses, etc., can, therefore, be exercised by proper viscoelastic material selection and temperature control (energy dissipation) and by advantageous positioning of diverse materials within the structure (VFGM). Optimum combined configurations can then be sought under prescribed constraints.

Failure probabilities and survival times or lifetimes based on specific failure theories are used as the ultimate constraints associated with VFGM designer materials. In the current instance, deterministic and stochastic failures based on developments in [33] are used to predict composite panel delamination failures. Additionally, time dependent stability criteria, such as creep panel flutter and buckling, are also considered. Of course, other constraints such as stress, strains, deformations, panel creep buckling and flutter times, etc., could also be prescribed.

Previous examples of aero-viscoelastic problems and structural control of lifting surface viscoelastic panels may be found in [34 – 39], where it is shown that viscoelastic flutter velocities may be smaller or larger than the corresponding elastic ones for identical geometries and mass distributions. Material capacity for increased damping, and hence energy dissipation, does not necessarily lead to higher flutter velocities. In these self-excited viscoelastic systems the answers lie in the phase relationships between inertia, aerodynamic and viscoelastic forces.

While the problem formulated and solved in this pilot study has input relating to lifting surfaces and aerodynamic noise, the analyses have with minor modifications equal applicability to acoustic and hydrodynamic noise in submarines and surface vessels as well as to ground transportation vehicles.

2. Analysis

2.1 General consideration

In a Cartesian system $x = \{x_i\}, i = 1, 2, 3$, consider a linear viscoelastic flat plate (panel) of constant mass m per unit length, thickness h and area $A = a * b$. The plate is subjected to lift due to airflow with free stream velocities U_r in the x_1-direction at an angle of attack α and due to motion contributions from the entire lifting surface as well as from plate deflections. Lift forces are further augmented by pressure fluctuations (aerodynamic noise) $\Delta p(x_1, x_2, t)$. The standard small deflection plate theory assumptions are applied and the linear viscoelastic constitutive relations are [40 – 42].

$$\sigma_{ij}(x,t) \;=\; \int_{-\infty}^{t} E^{*}_{ijkl}\,(\Xi)\,\epsilon_{kl}(x,t')\;dt' \;+\; \int_{-\infty}^{t} E^{*T}_{ij}\,(\Xi)\;\;\alpha T(x,t')\;dt' \tag{1}$$

or

$$\epsilon_{ij}(x,t) \;=\; \int_{-\infty}^{t} C^{*}_{ijkl}\,(\Xi)\,\sigma_{kl}(x,t')\;dt' \;-\; \int_{-\infty}^{t} C^{*T}_{ij}\,(\Xi)\;\;\alpha T(x,t')\;dt' \tag{2}$$

with

$$\Xi \;\equiv\; [x,t,t,'\,T(x,t'),\mathcal{F}(x,t')] \;=\; (x,t,t') \tag{3}$$

For isotropic materials, each set of the 36 E_{ijkl} and C_{ijkl} reduce to two functions each, while the E^T_{ij} and C^T_{ij} each coalesce into one other function. Alternately, the constitutive relations may be written in the form

$$\begin{aligned}\sigma_{ij}(x,t) \;&=\; E_{ijkl}(x,0)\;\epsilon_{kl}(x,t) \;+\; \int_{0}^{t} E_{ijkl}\,(\Xi)\,\frac{\partial \epsilon_{kl}(x,t')}{\partial t'}\;dt' \\ &+\; E_{ij}(x,0)\;\alpha T(x,t) + \int_{0}^{t} E^{T}_{ij}\,(\Xi)\,\frac{\partial\,[\alpha T(x,t')]}{\partial t'}\;dt' \end{aligned} \tag{4}$$

with similar expressions for the strains in terms of stresses. The Einstein tensor notation is used though out with repeated symbols in pairs indicating summations, while underscored indices denote lack of summations over their range. For an alternate formulation in terms of differential constitutive relations equations more suitable for Runge-Kutta approaches see Appendix A.

The $\mathcal{F}(x,t') \equiv \mathcal{F}_{ijkl}(x,t')$ functions describe VFGM influences on mechanical properties and may have anisotropic attributes in addition to their nonhomogeneous properties. The latter are prescribed by the creation of such properties through selected manufacturing processes and/or by material property dependencies on service temperatures. Thusly, anisotropic directionality may also be imposed, while temperature variations $T(x,t')$ are separately governed by thermal radiation, convection and/or conduction.

The elastic-viscoelastic correspondence principle (analogy) can be satisfied only if the constitutive relations (1) and (2) are convolution integrals, i.e. $E(\Xi) = E(x, t - t')$. The latter condition limits the functions to $\mathcal{F}(x)$ and $T(x)$ [25, 43] such that

$$\Xi \;=\; (x, t - t') \quad \text{if and only if} \quad \mathcal{F} = \mathcal{F}(x) \tag{5}$$

In other words, even if the later two functions are both separable, i.e. $\mathcal{F} = f_1(t) f_2(x)$ and $T = f_3(t) f_4(x)$, the hereditary constitutive relation integrals are still of the non-convolution type with $\Xi = (x, t, t')$. Furthermore, if the material exhibits any aging characteristics [44 – 47], which are by definition inherently time dependent, no correspondence principle can be achieved.

Additionally and independently, viscoelastic materials can exhibit other non-homogeneities and anisotropies due to mixture, multiple dissimilar materials, composite fibers, etc., as indicated by the explicit dependence of the relaxation moduli and creep compliances on x and/or t in Eqs. (1) and (2).

In the eventual total scheme of non-homogeneous, isotropic or anisotropic material properties in relation to stress, strain and deformation formulations all such contributions, whatever their sources, carry equal significance. Therefore, in analysis only specific spatial and temporal functionalities of each E_{ijkl} or C_{ijkl} count and their origins become blurred and indistinguishable. In other words, EFGM and VFGM and thermal property dependency problems fundamentally reduce to formulations and analyses associated with elastic and/or viscoelastic materials which have prescribed and distinct isotropic or anisotropic and non-homogeneous properties [25].

If one chooses a generalized Kelvin model (GKM) or any other mathematical, mechanical or electrical model to describe or simulate viscoelastic behavior, then the $\mathcal{F}$ and T functional dependence must be properly assigned to the individual parameters. In the case of varying temperatures, damping properties – i.e. damper viscosities – are heavily influenced while the model's elastic components are relatively insensitive to temperatures. However, these elastic contributions may have spatial inhomogeneities and anisotropies which are caused by FGMs but independent of temperatures.

Temperature and VFGM dependent and strain independent relaxation moduli can be expressed as Prony series [48]

$$\left\{ \begin{array}{c} E_{ijkl}(x,t) \\ \\ E^*_{ijkl}(x,t) \end{array} \right\} =$$

$$E_{ijkl\infty}(x,t) + \sum_{n=1}^{N_{\underline{ijkl}}} \left\{ \begin{array}{c} E_{\underline{ijkl}n}(x,t) \\ \\ \dfrac{E_{\underline{ijkl}n}(x,t)}{\tau_{\underline{ijkl}n}(x,t)} \end{array} \right\} \exp \underbrace{\left(\int^{t} \frac{-\, d\zeta}{\tau_{\underline{ijkl}n}\left[x, \zeta, T(x,\zeta), \mathcal{F}(x,\zeta)\right]} \right)}_{X_{\underline{ijkl}n}(x,t)} \tag{6}$$

with

$$E_{ijkl0}(x,t) \;=\; E_{ijkl\infty}(x,t) \;+\; \sum_{n=1}^{N_{\underline{ijkl}}} E_{\underline{ijkl}n}(x,t) \tag{7}$$

and where E_{ijkl0} are the equivalent anisotropic elastic moduli and τ_{ijkln} the relaxation times. When structural damping in the form of Coulomb friction [49] is included due to dissipation in joints, the elastic moduli can be modified to read $\left[1 + \imath\, g_{\underline{ijkl}}(x)\right] E_{\underline{ijkl}0}(x,t)$. The g_{ijkl} are called structural damping coefficients with a range of 0.005 to 0.05 [50]. It bears no relation to the gravitational constant universally designated by g. The relaxation moduli of Eqs. (6) may then be rewritten as

$$E_{ijkl}(x,t) \; = \; \Big[1 + \imath\, \underline{g_{ijkl}}(x)\Big]\, \underline{E_{ijkl0}}(x,t) \; + \; \sum_{n=1}^{N_{ijkl}} \underline{E_{ijkln}}(x,t) \Big\{ \exp\Big[\underline{X_{ijkln}}(x,t)\Big] \; - \; 1 \Big\} \tag{8}$$

Non-homogeneous properties can be achieved by either temperature dependent material properties, the presence of VFGM or both. Depending on the nature of the temperature and/or VFGM spatial functions, such nonhomogeneities may exist in either one or more x_i direction. Material time dependence is subject to the usual viscoelastic time functions plus any changes directly induced by temperatures and/or VFGMs. Viscoelastic plates will be exposed to (i) material failures in time and to instabilities such as (ii) creep flutter and/or (iii) creep buckling. Therefore, in order to define the failure primacy of any given panel, one needs to establish which of these three modes will occur first, and at what combinations of air speeds, frequencies and life or survival times.

For small deformations, the anisotropic, nonhomogeneous viscoelastic plate governing relation is given by

$$\begin{aligned}
\mathcal{L}(w, D^*, \mathcal{F}) \; = \; & \underbrace{\int_{-\infty}^{t} \left\{ \frac{\partial^2}{\partial x_1^2} \left(D^*_{1111} \left[\widehat{\Xi}\right] \frac{\partial^2 w(x,t')}{\partial x_1^2} \right) \; + \; 2\, \frac{\partial^2}{\partial x_1 \partial x_2} \left(D^*_{1212} \left[\widehat{\Xi}\right] \frac{\partial^2 w(x,t')}{\partial x_1 \partial x_2} \right) \right\} dt'}_{\text{viscoelastic bending resistance } (\mathrm{T_{1A}}\ \&\ \mathrm{T_{1B}})} \\
& + \underbrace{\int_{-\infty}^{t} \left\{ \frac{\partial^2}{\partial x_2^2} \left(D^*_{2222} \left[\widehat{\Xi}\right] \frac{\partial^2 w(x,t')}{\partial x_2^2} \right) \right\} dt'}_{\text{viscoelastic bending resistance } (\mathrm{T_{1C}})} \\
& - \left[\underbrace{\int_{-\infty}^{t} D^*_4 \left[\widehat{\Xi}\right] \left(\frac{\partial w(x,t')}{\partial x_1} \right)^2 dt'}_{\substack{\text{in plane force due to length change} \\ \text{in } \mathrm{x_1} \text{ direction } (\mathrm{T_2})}} + \underbrace{\mathcal{N}^{\mathbf{EX}}_{11}(x_2,t)}_{\text{external force } (\mathrm{T_3})} \right] \frac{\partial^2 w}{\partial x_1^2} \; + \; \underbrace{m_p \frac{\partial^2 w(x,t)}{\partial t^2}}_{\substack{\text{inertia effects} \\ (\mathrm{T_4})}} \\
& - \left[\underbrace{\int_{-\infty}^{t} D^*_5 \left[\widehat{\Xi}\right] \left(\frac{\partial w(x,t')}{\partial x_2} \right)^2 dt'}_{\substack{\text{in plane force due to length change} \\ \text{in } \mathrm{x_1} \text{ direction } (\mathrm{T_5})}} + \underbrace{\mathcal{N}^{\mathbf{EX}}_{22}(x_1,t)}_{\text{external force } (\mathrm{T_6})} \right] \frac{\partial^2 w}{\partial x_2^2} \\
& - \left[\underbrace{\int_{-\infty}^{t} D^*_6 \left[\widehat{\Xi}\right] \frac{\partial w(x,t')}{\partial x_1} \frac{\partial w(x,t')}{\partial x_2} dt'}_{\substack{\text{in plane force due to angle change} \\ \text{between } \mathrm{x_1}\ \&\ \mathrm{x_2} \text{ directions } (\mathrm{T_7})}} + \underbrace{\mathcal{N}^{\mathbf{EX}}_{12}(x_1,t)}_{\text{external force } (\mathrm{T_8})} \right] \frac{\partial^2 w}{\partial x_1 \partial x_2} \\
& - \left[\underbrace{\int_{-\infty}^{t} D^*_7 \left[\widehat{\Xi}\right] \frac{\partial w(x,t')}{\partial x_1} \frac{\partial w(x,t')}{\partial x_2} dt'}_{\substack{\text{in plane force due to angle change} \\ \text{between } \mathrm{x_1}\ \&\ \mathrm{x_2} \text{ directions } (\mathrm{T_9})}} + \underbrace{\mathcal{N}^{\mathbf{EX}}_{12}(x_2,t)}_{\text{external force } (\mathrm{T_{10}})} \right] \frac{\partial^2 w}{\partial x_1 \partial x_2}
\end{aligned}$$

$$+ \underbrace{a_0^*\, q\, \sin\left\{\frac{\pi}{2\,\alpha_{ST}}\left[\underbrace{\overbrace{\mathcal{A}_W(\alpha,\theta,W)}^{\substack{\text{wing contribution}\\ \text{Eq. (10)} \quad (\mathrm{T_{11W}})}} + \overbrace{\arctan\left(\frac{1}{U_r}\frac{\partial w(x,t)}{\partial t} + \frac{\partial w(x,t)}{\partial x_1}\right)}^{\text{panel contribution } (\mathrm{T_{11P}})}}_{\text{combined angle of attack due to deformed wing and panel}}\right]\right\}}_{\text{lift forces } (\mathrm{T_{11}})}$$

$$+ \underbrace{\mathcal{N}_{11}^{\mathbf{P}}(x,t)\frac{\partial^2 w}{\partial x_1^2}}_{\mathrm{x_1 \text{ piezo force } (T_{12})}} + \underbrace{\mathcal{N}_{22}^{\mathbf{P}}(x,t)\frac{\partial^2 w}{\partial x_2^2}}_{\mathrm{x_2 \text{ piezo force } (T_{13})}} + \underbrace{\mathcal{N}_{11}^{\mathbf{T}}(x,t)\frac{\partial^2 w}{\partial x_1^2}}_{\mathrm{x_1 \text{ thermal force } (T_{14})}} + \underbrace{\mathcal{N}_{22}^{\mathbf{T}}(x,t)\frac{\partial^2 w}{\partial x_1 \partial x_2}}_{\mathrm{x_2 \text{ thermal force } (T_{15})}}$$

$$+ \underbrace{2\,\mathcal{N}_{12}^{\mathbf{T}}(x,t)\frac{\partial^2 w}{\partial x_1 \partial x_2}}_{\substack{\text{thermal shear}\\ \text{force } (\mathrm{T_{16}})}} + \underbrace{\frac{\partial^2 M_{11}^{\mathbf{T}}}{\partial x_2^2}}_{\substack{x_3 \text{ load due}\\ \text{to } M_{11}^{\mathbf{T}} (T_{17})}} + \underbrace{\frac{\partial^2 M_{22}^{\mathbf{T}}}{\partial x_1^2}}_{\substack{x_3 \text{ load due}\\ \text{to } M_{22}^{\mathbf{T}} (T_{18})}} + 2\underbrace{\frac{\partial^2 M_{12}^{\mathbf{T}}}{\partial x_1 \partial x_2}}_{\substack{x_3 \text{ load due}\\ \text{to } M_{12}^{\mathbf{T}} (T_{19})}}$$

$$+ \overbrace{\underbrace{\frac{\partial^2 M_{11}^{\mathbf{E}}}{\partial x_2^2}}_{\substack{x_3 \text{ electric}\\ \text{load } (T_{21})}} + \underbrace{\frac{\partial^2 M_{22}^{\mathbf{E}}}{\partial x_1^2}}_{\substack{x_3 \text{ electric}\\ \text{load } (T_{22})}} + \underbrace{\frac{\partial^2 M_{11}^{\mathbf{M}}}{\partial x_2^2}}_{\substack{x_3 \text{ magnetic}\\ \text{load } (T_{23})}} + \underbrace{\frac{\partial^2 M_{22}^{\mathbf{E}}}{\partial x_1^2}}_{\substack{x_3 \text{ magnetic}\\ \text{load } (T_{24})}}}^{\text{electric and magnetic controls}} =$$

$$\underbrace{\Delta p\left(x, t, \overbrace{w, \frac{\partial w}{\partial x}, \frac{\partial^2 w}{\partial x \partial t}, \frac{\partial w}{\partial t}, \frac{\partial^2 w}{\partial t^2}}^{\text{plate contribution}}, \overbrace{\alpha, \theta, \frac{\partial \theta}{\partial t}, \frac{\partial^2 \theta}{\partial t^2}, W, \frac{\partial W}{\partial t}, \frac{\partial^2 W}{\partial t^2}}^{\text{wing contribution}}\right)}_{\text{aerodynamic noise pressure } (\mathrm{T_{20}})} \tag{9}$$

where the plate deflections are $w = w(x,t) = w(x_1,x_2,t)$ and the wing deflections are $\theta = \theta(x_2,t)$ and $W = W(x_2,t)$ unless otherwise indicated. In term $\mathrm{T_{11}}$, a_0^* is the slope of the lift curve, q the dynamic pressure and α_{ST} the stall angle.

In the absence of chord-wise bending the panel effective angle of attack due to wing contributions is

$$\mathcal{A}_W(\alpha,\theta,W) \;=$$

$$\underbrace{\overbrace{\alpha_r(x_2) - \alpha_0(x_2)}^{\substack{f_\alpha(x_2)=\text{built in}\\ \text{function}}} + \overbrace{\alpha(x_2)}^{\substack{\text{angle of}\\ \text{attack}}}}_{\text{rigid wing contributions}} + \underbrace{\overbrace{\theta(x_2,t)}^{\substack{\text{wing angle}\\ \text{of twist}}} + \overbrace{\arctan\left(\frac{1}{U_r}\frac{\partial W(x_2,t)}{\partial t}\right)}^{\text{wing bending velocity}}}_{\text{wing aero}-\text{viscoelastic contributions}} \tag{10}$$

and where

$$D_{ijkl}\left[\widehat{\Xi}\right] = \int_{-h/2}^{h/2} E_{ijkl}\left[\Xi\right]\, x_3^2\, dx_3 \qquad D_m\left[\widehat{\Xi}\right] = \int_{-h/2}^{h/2} E_{ijkl}\left[\Xi\right]\, dx_3$$

$$m = 4,5,6,7 \qquad \widehat{\Xi} \equiv [x,t,t', T(x,t'), \mathcal{F}(x,t')] = (x_1,x_2,t,t') \tag{11}$$

Eq. (9) represents the worst case aero-viscoelastic scenario where the lift T_{11} (including stall possibilities) and aerodynamic noise pressure T_{20} each are functions of wing and panel bending and twisting deflections. For isotropic materials, Eqs. (9) reduce in complexity as

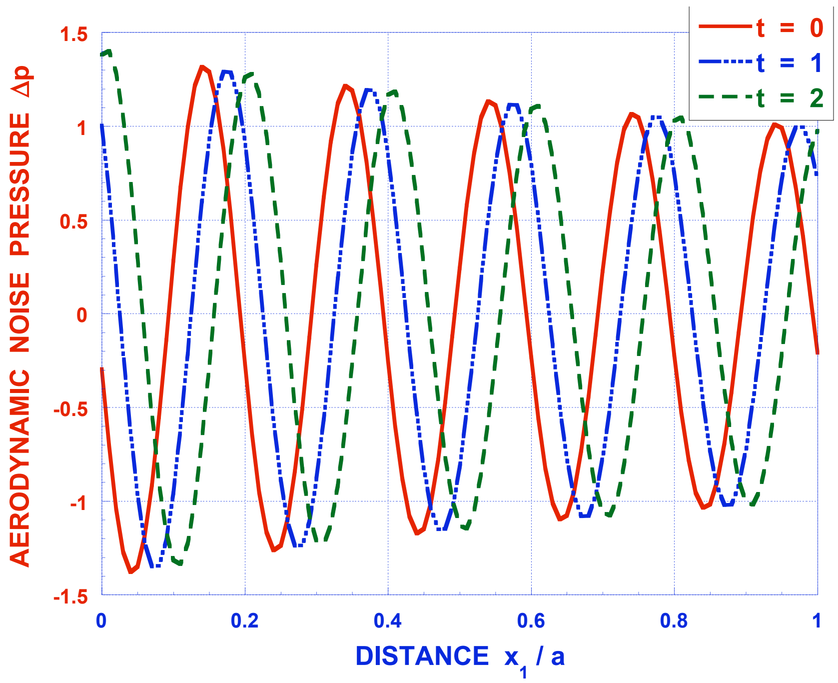

Figure 2: Sears [98] Aerodynamic noise spatial distributions

$$D \;=\; D_{\underline{iiii}} \qquad \text{and} \qquad D^* \;=\; D^*_{\underline{iiii}} \tag{12}$$

with similar equalities for the other rigidities D_m or D^*_m.

Thermal loads and moments are given by

$$\mathcal{N}^{\mathbf{T}}_{ij}\left[\widehat{\Xi}\right] \;=$$

$$\int\limits_{-h/2}^{h/2} \overbrace{\int\limits_{-\infty}^{t} E^{*T}_{ij}(\Xi)\;\alpha T(x,t')\;dt'}^{=\text{ thermal stresses }\sigma^{\mathrm{T}}_{\mathrm{ij}}}\;dx_3 \;=\; \int\limits_{-h/2}^{h/2} \overbrace{\int\limits_{-\infty}^{t} E^{T}_{ij}(\Xi)\;\frac{\partial\left[\alpha T(x,t')\right]}{\partial t'}\;dt'}^{=\text{ thermal stresses }\sigma^{\mathrm{T}}_{\mathrm{ij}}}\;dx_3 \tag{13}$$

$$M^{\mathbf{T}}_{ij}\left[\widehat{\Xi}\right] \;=$$

$$\int\limits_{-\infty}^{t}\int\limits_{-h/2}^{h/2} E^{*T}_{ij}(\Xi)\;\alpha T(x,t')\;x_3\;dx_3\;dt' = \int\limits_{-\infty}^{t}\int\limits_{-h/2}^{h/2} \frac{\partial\left[E^{T}_{ij}(\Xi)\;\alpha T(x,t')\right]}{\partial t'}\;x_3\;dx_3\;dt' \tag{14}$$

Aerodynamic forces are functions of angle of attack among other variables. With the flow parallel to the x_1–axis, angle changes will take place due to rigid and flexible plate motions. In particular, Sears' expression [98] in combination with flexible plate input, yields for small angles of attack

$$\underbrace{\Delta p(x,t)}_{\substack{\text{aero noise}\\(\mathrm{T}_{20})}} \;=\; \underbrace{\Re\left\{\Delta p^{Se}(x,t)\right\}}_{\substack{\text{rigid plate}\\(\mathrm{T}_{20\mathrm{RP}})}} \;+\; \underbrace{a^*_0\;q\left[\frac{\partial w(x,t)}{\partial x_1} \;+\; \frac{1}{U_r}\frac{\partial w(x,t)}{\partial t}\right]}_{\text{flexible plate with small angle of attack }(\mathrm{T}_{20\mathrm{FP}})} \tag{15}$$

where

$$\Re\left\{\Delta p^{Se}(x_1,t)\right\} \;=\; \frac{-\,\sqrt{2}\,\rho_0\,U_r\;a^*_3}{\sqrt{\pi\,\sigma_1(1+M_r)(\zeta+1)}}\;\otimes$$

$$\left\{\cos(\sigma_1 + k_1\,U_r\,t)\left[\cos\left(\frac{M_r\,\sigma_1}{1+M_r}(\zeta+1)\right) \;+\; \sin\left(\frac{M_r\,\sigma_1}{1+M_r}(\zeta+1)\right)\right]\right.$$

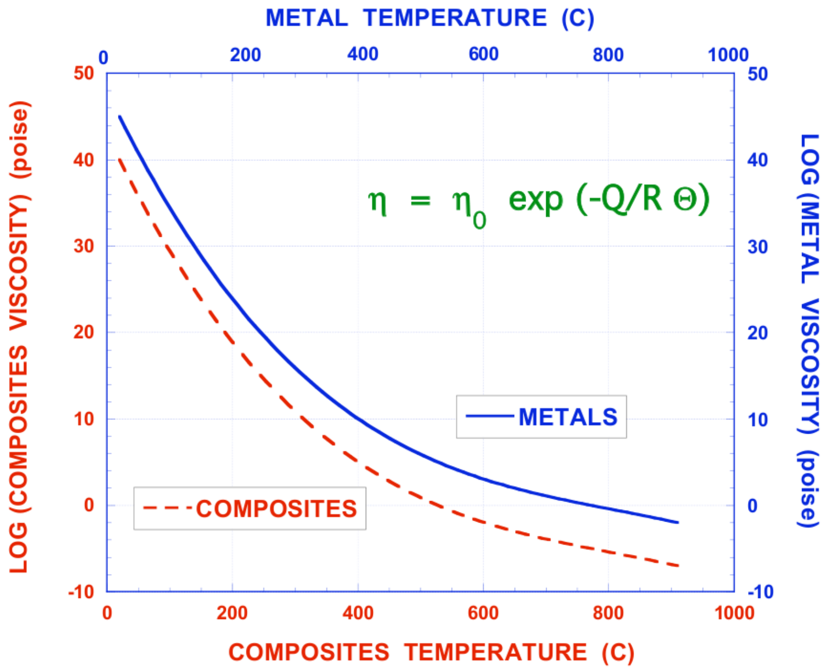

Figure 3: Coefficient of viscosity

Table 1: Influence of thermal expansions

Case	Thermal Expansion	End Restraints	Bending / Shear
A	$\alpha T(x_3, t)$	4 sides free	pure bending
B	$\alpha T(x_1, x_2, t)$	4 sides free	bending & shear
C	$\alpha T = const.$	x_3-direction motion at least one side restrained	bending & shear

$$+ \;\; \sin(\sigma_1 + k_1\, U_r\, t) \left[- \;\cos\left(\frac{M_r\, \sigma_1}{1 + M_r} (\zeta + 1) \right) \; + \; \sin\left(\frac{M_r\, \sigma_1}{1 + M_r} (\zeta + 1) \right) \right] \Bigg\} \tag{16}$$

Spatial distributions and time amplitudes of Δp^{Se}, Eq. (16), are displayed in Fig. 2 .

Inclusion of the flexible terms T_{20FP} above produces a self excited system where these additional contributions may be stabilizing or destabilizing depending on phase relations among the various terms of the governing equation (9). These terms combine with the corresponding first derivatives on the left hand side of (9) and modify their coefficients thereby fortifying or weakening stability boundaries.

Viscoelastic plate creep buckling theory has its roots in elastic column buckling analysis [51]. However, viscoelastic materials have memory and dissipate energy continuously in time and, therefore, the loading histories of all loads strongly influence the deformation path [52]. Consequently, Euler's lateral infinitesimal disturbance concept is inapplicable to columns and not needed for viscoelastic plates since they are exposed to lateral loads, such as T_{11} and T_{20}, producing deflections $w(x, t)$ for $t \geq 0$.

The relaxation moduli E and E^T are considered temperature dependent, thus rendering the material nonhomogeneous and effectively causing thermal gradients to generate a VFGM. The exceedingly strong temperature influence can be seem in Fig. 3, typically inducing one order of magnitude change in coefficients of viscosity per 20^o C. For thermo-rheologically simple materials (TSM) a shift function a_T may be introduced which in turn leads to a pseudo-

Table 2: Bending due to temperature distributions

Temperature Function $T(x_3,t)$	Relaxation Modulus $E[T(x_3,t)]$	Bending
even	even	no
even	odd	yes
odd	even	yes
odd	odd	yes

time ξ definition [40], [42]

$$\xi(x,t) \;=\; \int_0^t a_T\left[T(x,t')\right]\, dt' \tag{17}$$

and transforms all time integrals to convolution ones in the ξ-space, such that

$$\overline{\overline{\widehat{f}}}_1(x,\xi) \;=\; \int_{-\infty}^{\xi} \widehat{E}(x,\xi-\xi')\ \widehat{f}_2(x,\xi')\ d\xi' \;=\; \int_{-\infty}^{t} E(x,t,t')\ f_2(x,t')\ dt' \tag{18}$$

The shift function is generally expressed by [40], [42]

$$\log\left[a_T(T)\right] \;=\; \frac{-C_1\ (T\ -\ T_0)}{C_2\ +\ T\ -\ T_0} \tag{19}$$

where C_ns are material property parameters and T_0 a preselected reference temperature where $a(T_0)=1$. While this permits expressing viscoelastic material behavior in terms of master relaxation or compliance curves, it does not, however, allow the use of integral transforms (Laplace, Fourier, etc.) in the governing Eq. (9) when the temperature T is time dependent because of the influence of $\xi(x,t)$ on the x derivatives.

In small deformation column and plate theory one usually considers changes in length or width to be negligible and the instantaneous dimensions $L_i(t)$ in the x_i-directions remain equal to the original unloaded lengths L_i^0. If these changes become appreciable, then a nonlinear problem results.

If the in-planel loads $\mathcal{N}(t)$ and/or the thermal loads $\mathcal{N}^T$ remain normal to the cross section during bending deformations then in essence they are follower loads.

The plate length (width) changes due to in-plane loads are

$$L_{s_i}(t) \;=\; \int_0^t \int_0^{L_{s_{\underline{i}}}(t')} \frac{\mathcal{N}_{\underline{ii}}(s,'t') + \mathcal{N}^{\mathbf{T}}_{\underline{ii}}(s,'t')}{h}\ C_{\underline{ii}}[s,'t,t,'T(0,t')]\ ds'_{\underline{i}}\,dt' \tag{20}$$

with

$$\mathcal{N}_{ij} \;=\; \mathcal{N}^{\mathbf{EX}}_{ij} \;+\; \mathcal{N}^{\mathbf{P}}_{ij} \tag{21}$$

and where $C_{ij}(s,t)$ are the creep compliances of the plate material. The lengths $L_{s_i}(t)$ are due to compressive/tension loads and represent the distances along the deflected plate between its ends at the neutral axis in the s_i-directions. There are additional components due to bending given by

$$\int_0^{L_{\underline{i}}(t)} dx_{\underline{i}} \;=\; \int_0^{L^b_{s_{\underline{i}}}(t)} \sqrt{1-\left[\frac{dw(s,t)}{ds_{\underline{i}}}\right]^2}\ ds_{\underline{i}} \tag{22}$$

The unloaded length due to initial imperfections $w_0(s)$ is similarly given by

$$\int_0^{L_{\underline{i}}^0} dx_{\underline{i}} \;=\; \int_0^{L_{s_{\underline{i}}}^0} \sqrt{1 - \left[\frac{dw_0(s)}{ds_{\underline{i}}}\right]^2}\; ds_{\underline{i}} \tag{23}$$

If a plate end is free to move in the x_i-direction, then the corresponding $\mathcal{N}_{ij}^{\mathbf{T}}(t) = 0$. The thermal bending moment $M_i^T(t)$ is non zero only if the kernel of its integral is an odd function.

Viscoelastic initial conditions (IC) correspond to elastic solutions $w^E(x_1, x_2, t)$ at $t = 0$ of equivalent problems with identical $\mathcal{F}(x,t)$, $T(x,t)$ and boundary conditions (BC) at $s_i = 0$ and L_{s_i}, but with time independent elastic Young's moduli E^E. Elastic relations are then obtained from modifications of all above equations by the removal of all time integrals.

2.2 Deformations under pure thermal loads

It is, of course, possible to achieve a degree of passive control by material selection for best performance under independently mandated service temperatures. However, it must be noted that the presence of thermal expansions is generally accompanied by thermal stresses and strains and resulting in in plane thermal loads $\mathcal{N}^T$ as well as a high degree of material property dependence on temperature. Consider a loading configuration where the applied axial load $F(t) = 0$, the temperature is at most $T = T(t)$ with thermal loads $\mathcal{N}^{\mathbf{T}}(t) \neq 0$ and moments $M^{\mathbf{T}} = 0$ in Eqs. (13) and (14). Under these conditions $\mathcal{N}^T(t)$ and $w(s,t)$ may each increase or decrease depending on the nature of the relaxation moduli $E(x,t)$ time integrals. This deflection dichotomy has stability implications.

As a simple illustrative example let the temperature be

$$T(t) \;=\; \begin{cases} T_1 & \\ & 0 \le t \le \infty \qquad T_1,\ T_2 > 0 \\ \pm T_2\ t & \end{cases} \tag{24}$$

resulting in viscoelastic thermal loads $\mathcal{N}^{\mathbf{T}}$

$$\frac{\mathcal{N}^{\mathbf{T}}(t)}{\alpha\ A} \;=$$

$$\begin{cases} T_1\ E(t) \\ T_2\ \left(\pm\dfrac{E_\infty\, t^2}{2} \;+\; \displaystyle\sum_{n=1}^{N} E_n \left\{\tau_n^2 \left[\pm 1 \mp \exp\left(-\frac{t}{\tau_n}\right)\right] \mp t\ \tau_n \exp\left(-\frac{t}{\tau_n}\right)\right\}\right) \end{cases} \tag{25}$$

$$0 \le t \le \infty$$

which leads to exponentially decreasing $\mathcal{N}^{\mathbf{T}}$s for constant temperatures and a considerably more complicated thermal load for the second linearly increasing/decreasing temperature distribution (Fig. 4). Note that for the second temperature of Eq. (24) with a positive time rate, $\mathcal{N}^{\mathbf{T}} \ge 0$ starts out compressive in time, peaks and eventually becomes tensile for $T = T_2\, t$. This sign reversal is due to the fact that while T is increasing linearly in time, E decreases exponentially necessitating an end shortening recovery. Note the contrast in the behavior of the elastic equivalent $\mathcal{N}^{E\mathbf{T}}$ represented by the second pair of curves marked "EL". For time independent temperatures, $\mathcal{N}^{E\mathbf{T}}$ remains time invariant, while for temperatures with linear time variations $\mathcal{N}^{E\mathbf{T}}$ varies in like manner. This is due to the intrinsic definition of the elastic thermal loads as

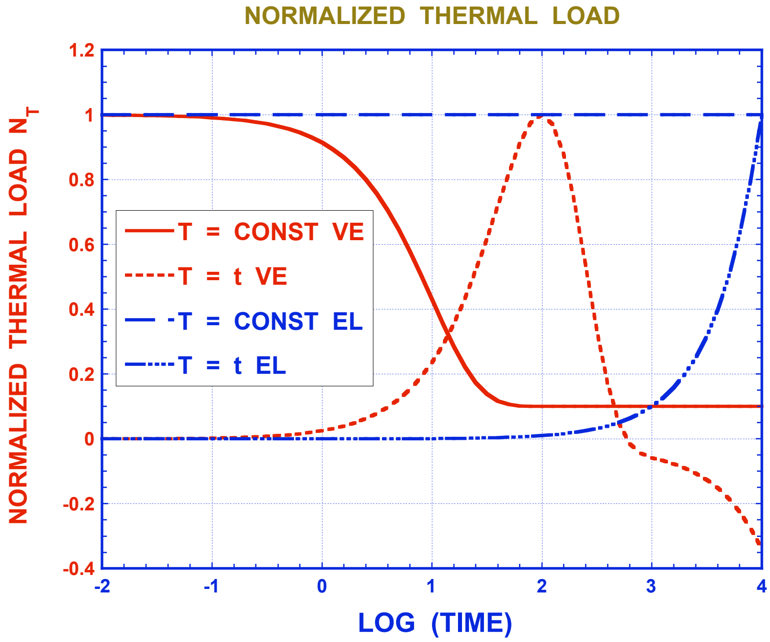

Figure 4: Thermal in-plane loads

$$\mathcal{N}^{E\mathbf{T}}(t) \;=\; E_0\,\alpha \int_{-h/2}^{h/2} T(x,t)\;dx_3 \qquad 0 \leq t \leq \infty \tag{26}$$

indicating that the the only time variation of $\mathcal{N}^{E\mathbf{T}}$ is due to $T(x,t)$.

Stability considerations and initial conditions dictate that

$$0 \;<\; \mathcal{N}^{\mathbf{T}}(0) \;<\; \mathcal{N}^{E}_{cr} \tag{27}$$

in order to allow creep deflection development with time. Of course, as seen from Tables 1 and 2, lateral plate deflections can be produced by $\mathcal{N}^{\mathbf{T}}(t) = 0$ and $M^{\mathbf{T}}(t) \neq 0$.

3. Creep buckling, flutter and failure analyses

The classical creep buckling definition is

$$\lim_{t \to t_{cr}} \{w(x,t)\} \;\to\; \infty \quad \text{or} \quad \lim_{t \to t^*_{cr}} \left\{ \frac{\partial w(x,t)}{\partial t} \right\} \;\to\; \infty \tag{28}$$

However, in Refs. [52] to [56] it has been shown that small deflection linear viscoelasticity analysis results in finite deflections for $0 < t_{cr},\ t^*_{cr} < \infty$. Consequently, alternate creep buckling definitions must be formulated. Two distinct types based on (1) strain reversal in time and (2) on time dependent material failure criteria have been offered.

In [57] it was proposed and successfully experimentally demonstrated that for elastic plates the buckling load can be established by analyzing graphs of outer plate fiber strains where compressive strains due loads and tensile strains due to bending take place. (See also [58] and [59] for comprehensive treatments of elastic and plastic buckling of thin-walled structures.) The elastic plate buckling load $\mathcal{N}^E_{cr}$ was defined as

$$\lim_{\mathcal{N} \to \mathcal{N}^E_{cr}} \frac{\partial \left[\epsilon^E_c(\mathcal{N}) + \epsilon^E_t(\mathcal{N}) \right]}{\partial \mathcal{N}} \;\to 0 \qquad t = 0 \tag{29}$$

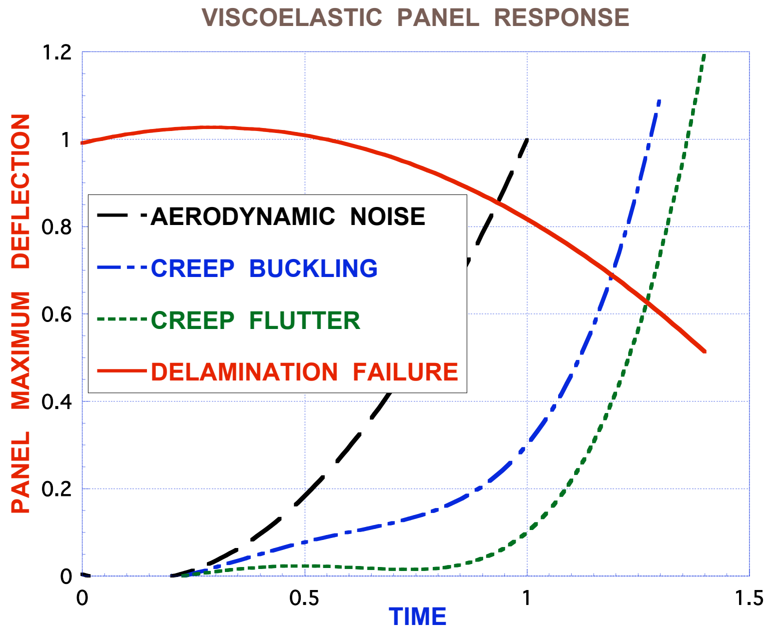

Figure 5: Viscoelastic buckling and flutter/divergence

This definition has been modified in Refs. [60] and [61] to read in the case of creep buckling as

$$\lim_{t \to t_{cr}^{\#}} \frac{\partial\left[\epsilon_c(t) + \epsilon_t(t)\right]}{\partial t} \to 0 \qquad 0 \leq \mathcal{N} < \mathcal{N}_{cr}^{E} \quad \text{and} \quad 0 < t_{cr}^{\#} < \infty \tag{30}$$

In the current case, one needs to change the $\mathcal{N}$ domain to $0 \leq \mathcal{N}_{11}(t) + N_{11}^{\mathbf{P}}(t) + N_{11}^{\mathbf{T}}(t) < \mathcal{N}_{cr}^{E}$ in order to incorporate piezoelectric and thermal load effects.

For a given lifting surface, flutter is defined in terms of two variables. namely flutter velocities V_F^E or Mach numbers M_F^E and frequencies Ω_F^E. In linear elastic and viscoelastic systems motion of the type

$$w_{max}(x,t) \;=\; \sum_{m=1}^{\infty} \exp\left\{\left[A_m(V,\Omega) + \imath\, B_m(V,\Omega)\right]\right\} t \tag{31}$$

is possible. In linear aeroelasticity one seeks eigenvalues for which $A(V_F, \Omega_F) = 0$, resulting in simple harmonic motion. The lowest value of V_F^E is known as the elastic flutter velocity.

Since the elastic solutions form viscoelastic initial conditions at $t = 0$, viscoelastic flutter at time $t = t_F$ can only occur at some $V_F < V_F^E$ when

$$\lim_{t \to t_F} w_{max}(x,t) \to \infty \qquad \text{or} \qquad \lim_{t \to t_F} \frac{\partial w_{max}(x,t)}{\partial t} \to \infty \tag{32}$$

This condition can be satisfied either by failure of the series to converge or by a single term becoming unbounded at $t = t_F$. A schematic comparison of creep buckling, flutter and structural-material failure is illustrated in Fig. 5 .

Viscoelastic failure criteria, such as ultimate stresses, degrade in time independently of relaxation moduli and failures may occur before or after any creep buckling instabilities manifest themselves. These are material failures which are independent of creep buckling and define the life time of the structure designated as t_{LF}. Consequently, t_{cr} or t_{cr}^{*} or $t_{cr}^{\#}$ may be greater, smaller or equal than t_{LF}. Indeed, in Refs. [52], [62] and [63] the Shanley & Ryder's [64] interaction curve approach has been used to estimate column failures under combined inelastic deterministic stresses.

Some failure mechanisms observed in composites are substantially different from those seen in metals as for example delamination which is a phenomenon unique to composites [65 – 70]. From a design analysis point of view, one needs only to consider delamination onset because at that stage a structure has for all practical purposes failed, particularly if it is a light weight flight structure. In [68] an expression has been formulated for the temperature, moisture and time dependency of uniaxial composite failure stresses. An extensive review of available experimental composite failure data is presented in [71] where such data is used to formulated deterministic and stochastic delamination failure analyses. Experimental results indicate that uniaxial deterministic delamination onset stresses in tension and shear obey laws of the type

$$\sigma_{ij}^{\mathbf{F}}(t) \;=\; \begin{cases} \sigma_{ij0}^{\mathbf{F}} & -\infty \leq t \leq t_2^{\mathbf{F}} \\ \sigma_{ij0}^{\mathbf{F}} \;-\; d_{ij}\;\log\left(t/t_4^{\mathbf{F}}\right) & t_2^{\mathbf{F}} \leq t \leq t_3^{\mathbf{F}} \\ 0 & t \geq t_3^{\mathbf{F}} \end{cases} \tag{33}$$

where all parameters are material, temperature, moisture and load (tension, shear, etc.) dependent (Fig. 8).

Failure criteria, however defined, are distinct from constitutive relations. For the purposes of the present analysis the combined load formulation of [33] in terms of stress invariants is used. The fundamental stress invariants for internal stresses are

$$J_1 \;=\; \frac{1}{3}\,\sigma_{ii} \qquad J_2 \;=\; \frac{1}{3}\,\sigma_{ij}\,\sigma_{ij} \qquad J_3 \;=\; \frac{1}{3}\,\sigma_{ij}\,\sigma_{ik}\,\sigma_{jk} \tag{34}$$

with similar expressions for failure stress invariants $\mathcal{J}_i$ in terms of uniaxial failure stresses σ_{ij}^F

$$\mathcal{J}_1 \;=\; \frac{1}{3}\,\sigma_{ii}^F \qquad \mathcal{J}_2 \;=\; \frac{1}{3}\,\sigma_{ij}^F\,\sigma_{ij}^F \qquad \mathcal{J}_3 \;=\; \frac{1}{3}\,\sigma_{ij}^F\,\sigma_{ik}^F\,\sigma_{jk}^F \tag{35}$$

The actual failure criteria are expressed as

$$\sum_{n=1}^{3}\left(\frac{\widetilde{J}_n}{\mathcal{J}_n}\right)^{c_n} \;=\; \widetilde{v} \qquad \text{and} \qquad \sum_{n=1}^{3}\left(\frac{\widetilde{\mathcal{J}}_n}{\mathcal{J}_n}\right)^{c_n} \;=\; \widetilde{V} \tag{36}$$

where $\widetilde{\ }$ indicate random variables and $\mathcal{J}_n$ are mean failure values. Failure will occur whenever

$$\widetilde{U} \;=\; \widetilde{V} - \widetilde{v} \;\leq\; 0 \tag{37}$$

Experimental results indicate that failure distributions are of the Weibull type [69], [72 – 74] thus defining probabilities of failure as

$$P_F(x,t) \;=\; 1 - \exp\left\{-\left[\frac{\widetilde{U}(x,t)}{\kappa}\right]^{\gamma}\right\} \tag{38}$$

where γ and κ are material property parameters. Since the stresses are functions of x and t, it follows that the failure probabilities P_F are also dependent on position within the plate and on time. The life or survival time t_{LF}, then, corresponds to the largest value P_F at a point $x_i = a_i$ in a plate is defined by

$$P_F(a, t_{LF}) \;=\; \max\left[P_F(x,t)\right] \;\leq\; 1 \tag{39}$$

In stochastic probabilistic structural failure analysis, one seeks similar points or regions where $P_F(x, t_{LF}) = 1$ or alternately the maximum probability value

$P_F(x, t_{LF}) < 1$ to indicate plate survival probabilities under a prescribed load $N(t) < N_{cr}^E$, the elastic critical load. The elastic critical load represents the upper bound of permissible viscoelastic loads since the initial conditions are elastic. A similar but distinct class of problems arises from the imposition of the specification of design survival times t_{LFD} each corresponding to a design failure probability $P_{FD}(t_{LFD}) \leq 1$, or conversely the prescription of a t_{LFD} with an attendant $P_{FD}(t_{LFD})$. It must, of course, also be remembered that the creep buckling times t_{cr} are unrelated to the survival times and each represents a distinct definition of instability or failure conditions.

In the final analysis combinations of probabilities of failure and survival times are the indicators of choice for geometric determinations and material selection.

4. Computational issues

The viscoelastic plate or panel governing relation (9), even in quasi-static or solely elastic configurations, are too complicated due to their nonlinear geometric nature to be reducible to analytical solutions and numerical protocols need to be applied. The various possibilities consist of:

- Reduction of spatial dependence through the application of collocation, Rayleigh-Ritz, Timoshenko, Galerkin or like methods [75]
- Subsequent solution of the time integral-differential relations by Runge-Kutta approaches [76].
- Alternately, finite element methods with numerical evaluation of the material property time integrals can be undertaken [77 – 85].
- Use of the general elastic-viscoelastic analogy as described in [40] is unachievable for time dependent temperatures $T(x, t)$ and FGMs $\mathcal{F}(x, t)$, unless the approximate correspondence principles of [86] and/or [87] are applied.

A solution of Eq. (9) presents special difficulties, in particular due to the presence of the time integral which does not allow an analytical solution as is the case for the nonlinear viscoelastic plate. A direct formal numerical approach necessitates the storage of all function values at all x_1 points for all preceding times. This is obviously uneconomical in terms of computer storage as well as computational real time usage and other approaches must be sought.

In connection with viscoelastic finite element analyses, a number of step by step time approximations for the evaluation of convolution and of non-convolution time integrals have been proposed [77 – 82]. These methods are summarized and compared in Ref. [83]. The advantage of these approaches is that only the previous time step needs to be retained for each time interval, thereby drastically reducing the needed computer memory and required computational time. The disadvantage lies in the close relation between accuracy and time step size. The accuracy can only be determined by varying the time step sizes and comparing results until "convergence" takes place. In Refs. [71] and [83] to [85] recurrence relations have been developed which involve only the two previous time steps and yield solutions which are markedly more accurate and require less CPU time than other methods.

In addition to the time integral computational difficulties, it must be remembered that the aero-viscoelastic panel problem is a self excited one due to the interactions and interdependence of aerodynamic forces and displacements [36]. Consequently, the latter must be continuously updated as the solution proceeds in real time.

4.1 Solution by Galerkin's method

Galerkin's method [75] consists of assuming expressions for the unknown functions with arbitrary coefficients where each term independently satisfies prescribed boundary conditions, such as for example

$$w(x_1, x_2, t) \;=\; \sum_{m=0}^{M} w_m(t)\; F_m(x_1, x_2) \tag{40}$$

Each function $F_m(x_1, x_2)$ satisfies all BCs identically for all $0 \leq m \leq M$ without constraining any of the amplitude functions $w_m(t)$.

For a plate with four sides simply supported, an appropriate expression for these functions is

$$w(x_1, x_2, t) \;=\; \sum_{m=1}^{M_w} \sum_{n=1}^{N_w} w_{mn}(t) \underbrace{\sin\left(\frac{(2\,m-1)\,\pi\,x_1}{a}\right) \sin\left(\frac{(2\,n-1)\,\pi\,x_2}{b}\right)}_{f_{mn}(x_1,x_2)} \tag{41}$$

Introducing expressions (41) into Eq. (9) and multiplying each term as indicated results in

$$\begin{aligned} w_{mn}(t) \int_0^a \int_0^b \sum_{k=1}^{M_w} \sum_{l=1}^{N_w} f_{mn}(x_1, x_2)\; \sin\left(\frac{(2\,k-1)\,\pi\,x_1}{a}\right) \sin\left(\frac{(2\,l-1)\,\pi\,x_2}{b}\right) dx_1 dx_2 \\ = \; w_{mn}(t)\; B_{mn} \qquad\qquad 1 \leq m \leq M_w \qquad 1 \leq n \leq N_w \end{aligned} \tag{42}$$

with similar expressions for the other terms of Eq. (9) involving x_1 and x_2 derivatives as well as time integrals and derivatives. Thus the system of governing partial-integral relations is reduced to $M_w \otimes N_w$ simultaneous second order ordinary integral-differential relations in the unknown functions $w_{mn}(t)$ which are amenable to solutions by finite difference approaches or Runge-Kutta methods.

Note from the discussion in the previous Section that changes in plate widths $L_{s_i}(t)$ and $L_i(t)$ of Eqs. (20) and (22) are part of the nonlinear solution and are, of course, heavily influenced by the BCs. However, if one assume no changes in width then, of course, the problem remains linear if additionally the in-plane forces T_5, T_7 and T_9 are also neglected in in the governing relation (9). However, it has been shown in [88 – 90] that these in plane forces strongly influence elastic flutter stability considerations.

4.2 Solution protocol

The general designer material protocol [19] consists of identifying the parameters to be optimized and of assembling the governing relations, the boundary and initial conditions and the desired constraints on the problem as shown schematically in the flow chart of Fig. 6 . The governing relations are solved analytically and spatial and temporal dependences are removed by suitable procedures leaving only the constant parameters as unknowns. The latter are then determined subject to the selected constraints using Lagrangian multipliers resulting in a combined optimized set.

The $\mathcal{F}(x)$ is an optimized spatial distribution function of properties for elastic (EFGM) or viscoelastic (VFGM) functionally graded materials, which can be represented, as a matter of convenience, in the closed domain of the deformable body by a Fourier series of the type

$$\mathcal{F}(x) \;=$$

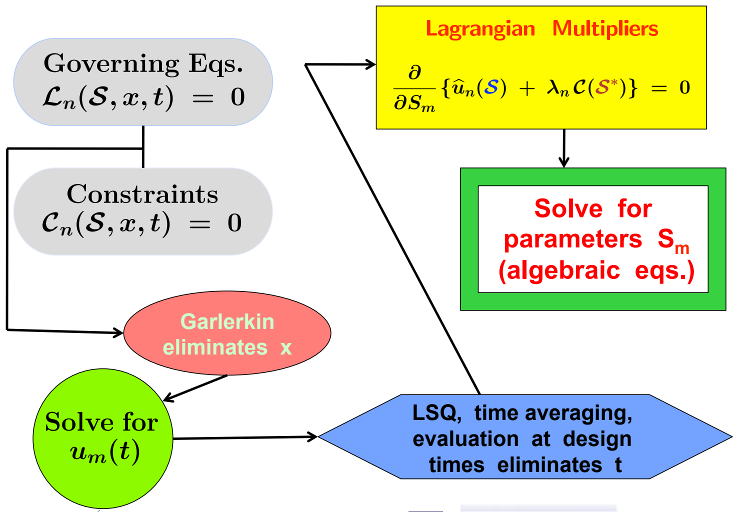

Figure 6: Designer material flow chart

$$\Re\left\{\sum_{\beta=1}^{B}\sum_{\gamma=1}^{\Gamma}\sum_{\mu=1}^{M} A_{\beta\gamma\mu}\exp\left[(b_\beta + \imath\, c_\beta)\, x_1\right]\exp\left[(b_\gamma + \imath\, c_\gamma)\, x_2\right]\exp\left[(b_\mu + \imath\, c_\mu)\, x_3\right]\right\} \tag{43}$$

where the A's maybe complex while the b's and c's are real. The optional presence of either FGM distributions can be used to further enhance the contributions of the optimized material properties and essentially renders the material non-homogeneous.

Designer materials, then, are in a class where the material property parameters E_{ijkln}, τ_{ijkln}, $A_{\beta\gamma\mu}$, b's and c's are optimized (tailored / engineered) simultaneously subject to pre-assigned constraints. For fiber–matrix composites, these parameters also include functions describing distributions of fiber orientations $\theta_{or}(x)$, number of plies $N_{pl}(x)$, number of fibers per ply $N_{fp}(x)$, volume fractions $v_{fr}(x)$ and stacking sequences $st(x)$. These composite related functions can be incorporated into the VFGM function $\mathcal{F}(x)$ of Eq. (43) above or treated as separate functions or as additional constraints, such as

$$\mathcal{C}_C\left[\theta_{or}(x), N_{pl}(x), N_{fp}(x), v_{fr}(x), st(x)\right] \;=\; 0 \tag{44}$$

In either manner appropriate additional parameters are created for these composite functions.

This parameter set is generically designated as $\boldsymbol{S} = \{S_1, S_2, \cdots, S_\kappa\}$ and all S_p are constants. Additionally, some of these properties may also be spatially optimally distributed throughout part or all of the structure to obtain still greater performance, cost permitting.

The behavior (response) of any deformable body problem is defined by one or more governing relations[1]

$$\mathcal{L}_\ell\left(x, t, \boldsymbol{S}, \boldsymbol{u}\right) \;=\; 0 \qquad \ell = 1, 2, \cdots, L \tag{45}$$

with L number of solution functions

$$\boldsymbol{u} = \boldsymbol{u}\left(x, t, \boldsymbol{S}\right) = \{u_1(x, t, \boldsymbol{S},), u_2(x, t, \boldsymbol{S}), \cdots, u_L(x, t, \boldsymbol{S})\} \tag{46}$$

which depend on body geometry, type of loads, boundary and initial conditions, etc. These governing relations are not necessarily limited to structural considerations alone, but could also describe for instance in the case of a flight vehicle the pertinent aerodynamics, stability and control, mission requirements, etc., [19].

[1] For the present problem the $\mathcal{L}$ function is defined by Eqs. (9).

The governing relations may also be subject to any number of constraints, which can be written symbolically as

$$\mathcal{C}\Big(\mathcal{WEIGHT}, \mathcal{DIMENSION}, \mathcal{MORPHING}, \mathcal{COST}, \mathcal{FAILURE}, \\ \mathcal{STABILITY}, \mathcal{CONTROL}, \cdots, x, t, S_1, S_2, \cdots, S_\kappa, \boldsymbol{u}\Big) = 0 \qquad (47)$$

One or more constraint function $\mathcal{C}$ may be defined or prescribed.

The now augmented number of parameters S_p for $p = 1, 2, \cdots, \kappa, \kappa{+}1, \cdots, \mathcal{K}$ are constants and the following solution protocol may be adopted:

1. Since the parameters $\mathcal{S}$ and the solution functions u_ℓ are unknown, all solutions must be formulated analytically, except for the final steps (Step 5 below) where the $\mathcal{S}$ parameters are determined.

2. Use Galerkin's approach to determine the coefficients of the series solutions to the governing relations $\mathcal{L}_\ell$

$$u_\ell(x, t, \boldsymbol{S}) = \sum_{k=1}^{\overline{K}} \sum_{l=1}^{\overline{L}} \sum_{m=1}^{\overline{M}} B_{\ell klm}(t, \boldsymbol{S})\, f_{\ell k}(x_1)\ f_{\ell l}(x_2)\ f_{\ell m}(x_3) \qquad (48)$$

where each and every function $f_{\ell k}, f_{\ell l}$ and $f_{\ell m}$ identically satisfies the boundary conditions. This procedure eliminates the x dependence of the governing relations (45) to either integral-differential relations or ODEs in time, such that

$$\widehat{\mathcal{L}}_\ell\left[t, \boldsymbol{S}, \boldsymbol{B}(t, \boldsymbol{S})\right] = \\ \int_V \mathcal{L}_{\underline{\ell}}\left[x, t, \boldsymbol{S}, \boldsymbol{u}(x, t, \boldsymbol{S})\right]\, f_{\underline{\ell}k}(x_1)\ f_{\underline{\ell}l}(x_2)\ f_{\underline{\ell}m}(x_3)\ dV = 0 \qquad (49)$$

with $\boldsymbol{B}(t, \boldsymbol{S}) = \{B_{\ell klm}(t, \boldsymbol{S})\}$, corresponding to $\widehat{u}_\ell(t, \boldsymbol{S})$, which results from boundary conditions and the Galerkin integrals based on the original governing relations (45).

3. Solve Eqs. (45) analytically and simultaneously to determine the $L \otimes \left(\overline{K} + \overline{L} + \overline{M}\right)$ number of functions $B_{\ell klm}(t, \boldsymbol{S})$.

4. Eliminate the time variable t by an averaging or similar process

$$\widetilde{u}_\ell(\boldsymbol{S}) = \int_0^{t_{max}} \frac{\widehat{u}_\ell(t, \boldsymbol{S})\ dt}{t_{max}} \qquad (50)$$

where t_{max} is the largest expected cumulative operational time, i.e. the lifetime of a component or a subsection such as a lifting surface or the entire vehicle.

Alternately, the time variable may be referenced to a a specific time $\widetilde{t}$ such as when the deflections reach a global maximum at one $\widehat{u}_\ell(t, \boldsymbol{S})$

$$\max\left\{\widetilde{u}_\ell(\boldsymbol{S})\right\} = \widehat{u}_\ell(\widetilde{t}, \boldsymbol{S}) \qquad (51)$$

Other procedures for eliminating time at this point in the analysis, such as for instance least squares or collocation, also can be used. In the case of flutter where the solutions are harmonic in time, the exponential functions divide out in any linear system and the time dependence is automatically removed from Eqs. (52).

5. Employ Lagrange multipliers to solve for the unknown parameters S_p from the $\mathcal{K} + L_q$ simultaneous relations

$$\frac{\partial}{\partial S_p}\Big\{ \sum_{\ell=1}^{L} \widetilde{u}_\ell(\boldsymbol{S}) \;+\; \lambda_q \, \widetilde{\mathcal{C}}_q(\boldsymbol{S}) \Big\} \;=\; 0 \tag{52a}$$

or

$$\frac{\partial}{\partial S_p}\Big\{ \sum_{\ell=1}^{L} \widetilde{u}_\ell(\boldsymbol{S}) \;+\; \lambda_1 \sum_{q=1}^{L_q} \widetilde{\mathcal{C}}_q(\boldsymbol{S}) \Big\} \;=\; 0 \tag{52b}$$

with $\qquad p = 1, 2, \cdots, \mathcal{K} + L_q \qquad \ell = 1, 2, \cdots, L$

and $\qquad \boldsymbol{S} = \{S_p\} = \{ \underbrace{S_1, S_2, \cdots, S_{\mathcal{K}},}_{\text{material, control and constraint parameters}} \overbrace{\lambda_1, \cdots, \lambda_{L_q}}^{\text{Lagrangian multipliers}} \}$

The individual Lagrangian multiplier λ_q are a most important part of the solution process itself as they act as "catalysts." However, their actual values are unimportant as only the S_p parameters dealing with properties, constraints and controls[2] are sought for $1 \leq p \leq \mathcal{K}$. The original differential-integral governing relations (45) have now been reduced to a coupled system of $\mathcal{K} + L_q$ simultaneous ones in the unknown parameters S_p, $(1 \leq p \leq \mathcal{K} + L_q)$, which are at best algebraic and at worst transcendental.

5. Discussion

For the thin plates once the thickness h is agreed upon, the possibility of substantial contributions due to controlled variations of properties in the thickness x_3-directions is practically nil. This is due to the fact that any such variations are "smoothed over" by the application of plane stress theory as exemplified by the integrals of Eqs. (11) defining the D bending rigidities. A self-evident protocol calls for having as much structural material as far away as possible form the neutral surface (NS) in order to produce the strongest and lightest plate. In viscoelastic symmetric or un-symmetric bending the NS – not necessarily a plane – with coordinates $x_i = c_i$ is defined by

$$\epsilon_{11}(c,t) \;=\; \epsilon_{22}(c,t) \;=\; 0 \qquad \text{on the NS} \tag{53}$$

where $\epsilon_{\underline{ii}}$ are the total strain components. It has been in shown in [91] that for bending of cross sections with nonhomogeneous materials the NS will translate and rotate in time relative to its initial ($t = 0$) elastic position, thus further complicating optimum material selections which now become time sensitive. While such optimal time functions are mathematically definable, they are practically unrealistic since it is difficult to produce such prescribed FGMs in time. However, this type of analysis is most useful in establishing upper and lower property bounds [25].

Composite plates on the other hand, because of fiber ply orientations, number and type of fibers in each ply, etc., inherently carry the possibility of fixed material property optimization to satisfy *a priori* time independent constraints. The latter can be represented by, but are not limited to, one or more of the following: minimizing stresses, strains, displacements and failure probabilities, or maximizing survival or life times.

Material property variations in the in-plane directions x_1 and x_2 directions, inherently possess more pronounced capabilities to influence the constraints

[2] As defined by Eqs. (1) - (3) for constitutive relations, (43) for VFGM, (47) for constraints.

mentioned previously. As an illustration consider the identical isotropic rectangular plate but with the x_1 edges simply supported and both x_2 ones free. Eq. (41) then becomes

$$w(x_1,t) \;=\; \sum_{m=1}^{M} w_m(t)\ \sin\left(\frac{(2\,m-1)\,\pi\,x_1}{a}\right) \qquad 0 \le x_1 \le a \tag{54}$$

After application of Galerkin's protocol, the governing relation (9) is reduced to a set of ODEs in time only. In its simplest linear form with only terms T_1, T_4, $T_{11\mathrm{P}}$ and T_{20} present, it reads

$$\underbrace{A_{2m}\frac{d^2 w_m}{dt^2}}_{\text{inertia }(\mathrm{T}^{\mathrm{G}}_{4\mathrm{m}})} + \underbrace{A_{1m}\frac{dw_m}{dt} + A_{0bm}\,w_m}_{\text{lift force on plate }(\mathrm{T}^{\mathrm{G}}_{11\mathrm{mP}})} + \underbrace{\int_{-\infty}^{t} A_{0am}(t,t')\,\frac{\partial w_m(t')}{\partial t'}\,dt'}_{\text{viscoelastic resistance force }(\mathrm{T}^{\mathrm{G}}_{1\mathrm{m}})} =$$

$$\underbrace{\Delta p_m(t)}_{\substack{\text{aerodynamic}\\ \text{noise }(\mathrm{T}^{\mathrm{G}}_{20\mathrm{m}})}} \qquad 1 < m \le M_w \tag{55}$$

with the integral terms T^G_{1m} reflecting viscoelastic material property contributions influenced by VFGM $\mathcal{F}$ and temperature T functions.

The influence of VFGMs and temperatures on material properties – relaxation moduli, Eq. (6) – manifests itself in three ways: (i) Equal changes in all relaxation times τ_n resulting in left or right shifts of the modulus curves relative to the time scale and curves maintain their shape, (ii) Changes in coefficient E_n producing different curve shapes and (iii) Combinations of (i) and (ii). In elastic materials increases in modulus values lead to decreases in displacements and increases in response frequencies. In viscoelastic materials, the effect cannot be generalized since it depends on the response-time paths defined by the specific characteristics of the integro-differential relation (55) and must be examined in a case by case manner.

For the conditions where both $\mathcal{F}$ and T are time independent functions, the integrals T^G_{1m} reduce to convolutions ones and Fourier transforms (FT) can be used to solve Eqs. (55), to yield upon inversion

$$\overline{\overline{w}}_m(\omega) \;=\; \frac{\overline{\overline{NU}}_m(\omega)}{\overline{\overline{DE}}_m(\omega)} \;=\; \overline{\overline{D^*}}_m(\omega)\ \overline{\overline{N}}_m(\omega) \qquad \Longrightarrow$$

$$w_m(t) \;=\; \int_{-\infty}^{t} D^*_m(t-t')\ NU_m(t')\ dt' \tag{56}$$

where the time functions are the FT inverses of

$$\overline{\overline{NU}}_m(\omega) \;=\; \overline{\overline{\Delta p}}_m(\omega) + A_{2m}\left[\imath\,\omega\,w_m(-\infty) \;+\; \dot{w}_m(-\infty)\right] + A_{1m}\,w_m(-\infty) \tag{57}$$

$$\overline{\overline{DE}}_m(\omega) \;=\; -\,\omega^2\,A_{2m} \;+\; \imath\,\omega\,A_{1m} \;+\; A_{0bm} \;+\; \overline{\overline{A}}_{0am}(\omega) \tag{58}$$

with from (6)

$$\overline{\overline{A}}_{0am}(\omega) \;=\; \overline{\overline{A}}_{m\infty} \;+\; \sum_{n=1}^{N}\overline{\overline{A}}_{mn}\,(\omega,T,\mathcal{F}) \tag{59}$$

The initial conditions (ICs) are taken with the understanding that state variables such as for instance $u_m(t)$ are at rest at $t=-\infty$. These conditions cannot be met by steady state SHM for $t\in[-\infty,\infty]$. However it has been shown in [92] that properly posed viscoelastic problems, because of their memory

$\overline{\overline{\overline{DE}}}_m$	Deflection	Action
$\dfrac{B}{(\imath\,\omega)^n}$	$\dfrac{(n-1)!}{B\,t^n}$	For larger B & n, $w(t)$ decreases
$\dfrac{B}{\imath\,\omega \pm 1/\tau_n}$	$\dfrac{\tau_n \exp\left(\mp t/\tau_n\right)}{B}$	For larger B & τ_n, $w(t)$ decreases

Table 3: The influence of VFGMs on deflections

capabilities, cannot admit non zero force and displacement ICs. Therefore, for SHM to be achieved proper initial buildup protocols must be prescribed.

A parametric study can now be undertaken regarding the effects of VFGM functions $\mathcal{F}$ on the $w_m(t)$s. Consider the influence of increasing $\overline{\overline{D}}_m \propto \int \overline{\overline{E}}(x_1, \omega)\, f_m(x_1)\, dx_1$ on the deflection component $w_m(t)$ for $\Delta p_m(t) = \text{const}$. Of course, for decreasing $\overline{\overline{\overline{DE}}}_m$s the converse is equally applicable as the reverse action ensues.

The next step is to take the results of Table 3 and translate them to the VFGM function $\mathcal{F}$ as indicated in Eqs. (6), (11) and (42) to produce the "largest" $\overline{\overline{A}}_{0mn}$ and hence the "largest" $\overline{\overline{D}}_m$ in (58). The individual m FT terms of T^G_{1m} become

$$\overline{\overline{A}}_{0am}(\omega) = \int_0^a \sum_{n=1}^{N} \frac{E_n(x_1)}{\imath\,\omega + 1/\tau_n(x_1)} \sum_{k=1}^{M_w} \sin\left(\frac{(2\,m-1)\,\pi\ \ x_1}{a}\right)\ \sin\left(\frac{(2\,k-1)\,\pi\ \ x_1}{a}\right)\ dx_1$$

$$1 \le m \le M_w \tag{60}$$

The E_n and τ_n dependencies on x_1 are due to the VFGM function $\mathcal{F}(x_1)$ that one would like to tailor to produce a "large" $\overline{\overline{E}}(x_1, \omega)$ and consequently a "small" $w(x_1, t)$. Unfortunately there is no known protocol to effect such a solution directly. One must, therefore, use an inverse approach of *a priori* $\mathcal{F}$ function selections, evaluate (60) and compare the results from (56). One approach is to solve for the plate deflections with homogeneous material properties and note the regions where maximum stress, deformation, etc., values take place. These regions are, of course, also dependent on the aerodynamic noise $\Delta p(x_1, x_2, t)$ and in-plane loads $\mathcal{N}_{ij}(x_1, x_2, t)$ acting on the panel. Traveling waves from $0 \le x_1 \le a$ will induce spatial and temporal moving maximum wave amplitudes as can be seen in Fig. 2 . Even in the deterministic aerodynamic noise loading as exemplified by the Sears model [98] the maximum amplitude panel location of the noise moves in time relatively gently compared to the random waves of Fig. 7 .

Once these regions are identified on the panel, one can then attempt to locally reinforce the plate with VFGMs in those regions and thus produce larger effective $E_{ijkl}(x, t)$ with proper spatial and/or temporal distributions tailored to reduce deformations $w(x_1, x_2, t)$ resulting in lighter structures. Alternately, material properties could be tailored to reduce failure probabilities, retard creep rates, increase lifetimes, etc., or their combinations as constraints.

A more general solution involving BCs with at least three restrained sides is depicted in Fig. 9, where failure probabilities are the constraints. For a prescribed set of delamination properties as exemplified by those of Fig. 8, designer relaxation moduli with optimum regional properties as defined in Fig. 1 are

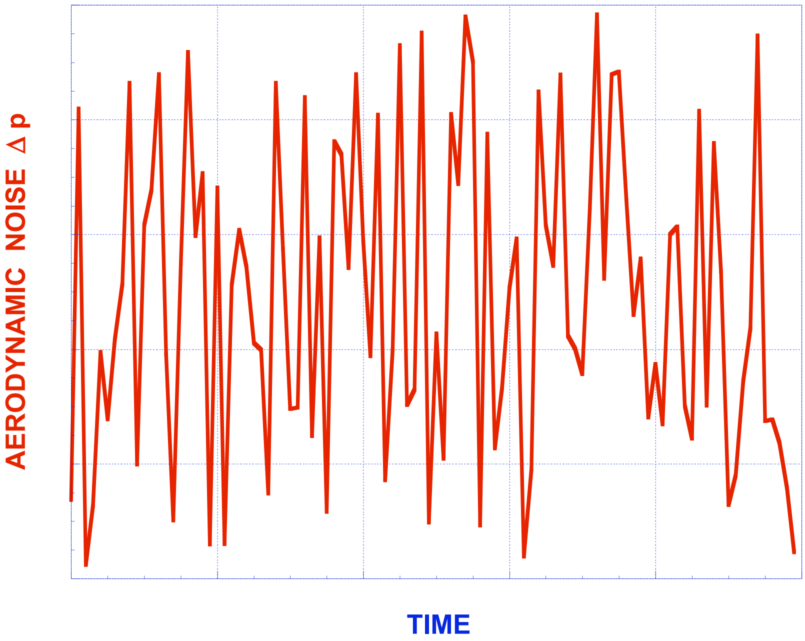

Figure 7: Random aerodynamic noise time distribution

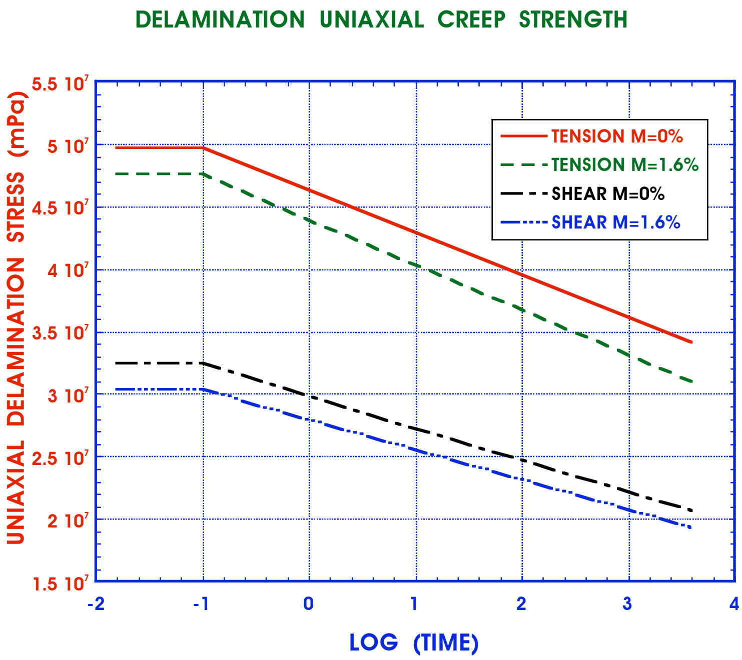

Figure 8: Uniaxial delamination creep strength [68]

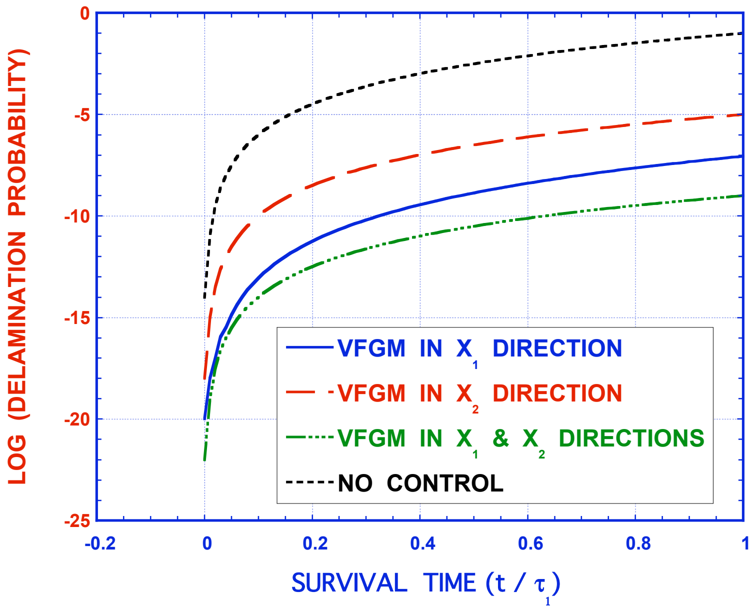

Figure 9: VFGM delamination probabilities

sought through an inverse trial and error approach. Fig. 9 indicates that better and more effective reductions in failure probabilities can be realized through spatial property variations in both x_1 and x_2 directions rather than in either one direction separately.

Fig. 9 is representative of the ultimate resolution of the posed problem, i. e. reduction of failure probabilities to prescribed levels and/or extension of structural lifetimes past expected service lives. This can be accomplished in combination of (A) the judicious imposition of designer material properties, (B) the distribution of appropriate non-homogeneous moduli (VFGM) and (C) the selection of materials with advantageous failure envelopes. As the largest deformations and stresses occur in the region of $0 \leq x_1 \lessapprox .1$, VFGM improvements need to be accentuated there.

However, the underlying caveat to remember is that in self-excited systems changes made intuitively in open loop systems may be destructive to closed ones, i. e. more damping or increased stiffness will not necessarily improve stability, failure or other critical conditions. Ultimately, aero-viscoelastic and aeroelastic responses and behavioral patterns revolve primarily around phase relationships between all aerodynamic, inertia, material, structural and applied contributory forces.

Before closing, a more detailed examination of Fig. 10 is required. Here the normalized deflections at the plate center are plotted against time in seconds. Since Galerkin's method is numerical no analytical convergence of the series Eq. (41) can be undertaken. Convergence is, therefore, established by taking successive numbers of terms for $w(x, t)$ and comparing results in regions where large deformations occur until no further changes are observed. The curves are for 1 (black), 4, 9 and 25 (red) terms. As seen in Fig. 10, twenty-five terms yielded stabilized deflection results. The symbolic Galerkin integral evaluations and all computations were carried out on a PC using MATLAB™.

6. Conclusions

The following observations emerge from this study:

- EFGM and VFGM problems fundamentally reduce to formulations and

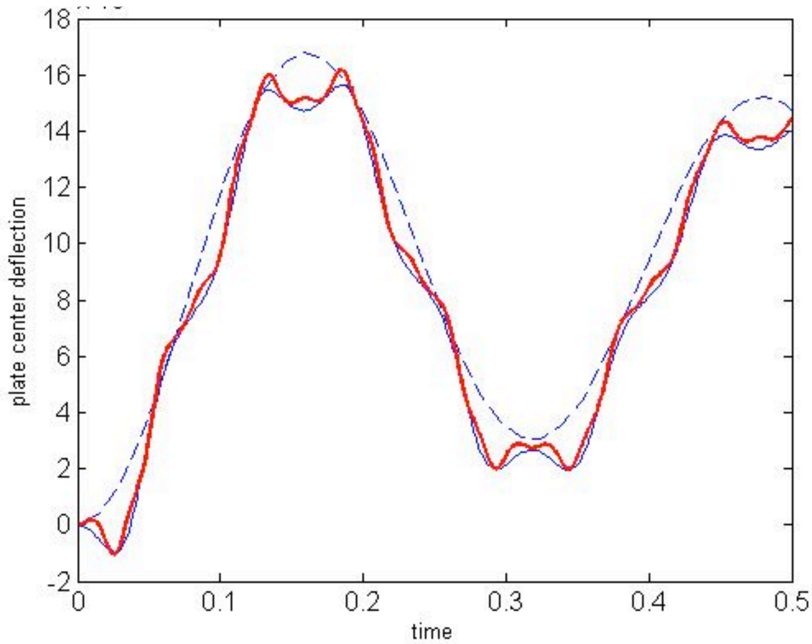

Figure 10: Galerkin convergence

analyses of elastic and viscoelastic materials having prescribed distinct isotropic or anisotropic and non-homogeneous properties.

- The strong dependence of viscoelastic material properties on temperature causes thermal gradients to generate *de facto* VFGM conditions.
- Viscoelastic axial thermal loads produced by boundary conditions and thermal expansions radically differ from their elastic counterparts in magnitude as well as in time histories.
- Higher temperatures degrade relaxation moduli and failure properties earlier and, therefore, reduce plate lifetimes as well as augmenting failure probabilities.
- Temperature distributions with or without boundary constraints can generate sufficiently large thermal bending deformations and stresses to cause time dependent creep buckling and/or material failures without the presence of additional axial compressive loads. This is a condition of pure thermal creep buckling.
- VFGM distributions in the thickness direction have limited utility because of plate thinness, except for tension relief. However, judicious in-plane distributions of VFGM can produce appreciable structural performance enhancements and contribute to structural weight reductions.
- Selected temperature and/or VFGM distributions may stabilize motion or extend dynamic plate lifetimes provided phase relationship are properly altered to dissipate additional energy or beneficial axial thermal loads are induced in opposition to the applied compressive in-plane plate loads. However, ultimately the plate will fail in time unless its motion is totally damped out before such failure envelopes are reached.
- In the final analysis, viscoelastic plates with materials that are less sensitive under combined loads to either or both relaxation moduli or failure property degradations will survive longer at lower failure probabilities.
- The ultimate purpose of the described inverse protocol is to design materials based on their properties and tailored to specific tasks, rather than conventional design of structures and/or their components.

Acknowledgments

Support by grants from the Technology Research, Education and Commercialization Center (TRECC) and Private Sector Program (PSP) Division both of the National Center for Supercomputing Applications (NCSA) at the University of Illinois at Urbana-Champaign (UIUC) and from the NASA NNG05GE81H Undergraduate Research Opportunities Program (UROP) is gratefully acknowledged.

References

[1] B. J. Lazan. *Damping of Materials and Members in Structural Mechanics.* Pergamon Press, Oxford, 1968.

[2] A. D. Nashif, D. I. G. Jones and J. P. Henderson. *Vibration Damping.* John Wiley & Sons, New York, 1985.

[3] D. I. G. Jones. *Handbook of Viscoelastic Vibration Damping.* John Wiley & Sons, New York, 2001.

[4] W. G. Buttlar, E. V. Dave, H. H. Hilton and G. H. Paulino. "Viscoelastic functionally graded materials: theory and applications," in press *Applied Mechanics Reviews*, 2012.

[5] H. H. Hilton and M. Feigen. "Minimum weight analysis based on structural reliability," *Journal of the Aero/Space Sciences*, 27:926–934, 1960.

[6] P. M. Weaver and M. F. Ashby. "The optimal selection of material and section shape," *Journal of Engineering Design*, 7:129–150, 1996.

[7] S. L. Lemanski and P. M. Weaver. "Analytical optimisation of composite cylindrical shells to meet given cross-sectional stiffness properties," *Proceedings 44th AIAA/ASCE/ASME/AHS SDM Conference*, Norfolk, VA, 2003.

[8] L. Cecchini and P. M. Weaver. "The optimisation of foam-filled cylindrical shells subject to flexural loading," *Proceedings 44th AIAA/ ASCE/ASME/AHS SDM Conference*, Norfolk, VA, 2003.

[9] P. M. Weaver. "On optimization of long anisotropic flat plates subject to shear buckling loads," *Proceedings 45th AIAA/ASCE/ASME/ AHS SDM Conference*, Palm Springs, CA, 2004.

[10] S. L. Lemanski and P. M. Weaver. "Optimization of a 4-layer laminated cylindrical shell to meet given cross-sectional stiffness properties," *Composite Structures*, 72:163–176, 2006.

[11] J. E. Herencia, P. M. Weaver and M. I. Friswell. "Optimization of long anisotropic laminated fiber composite panels with T-shaped stiffeners," *AIAA Journal*, 45:2497–2509, 2007.

[12] J. E. Herencia, P. M. Weaver and M. I. Friswell. "Optimization of anisotropic plates that vary in thicknesses and properties," *Proceedings 16th International Conference on Composite Materials*, Kyoto, Japan, 2007.

[13] J. E. Herencia, P. M. Weaver and M. I. Friswell. "Local optimization of anisotropic composite panels with T-shape stiffeners," *Proceedings 48th AIAA/ASCE/ ASME/AHS SDM Conference*, Waikiki, HI, 2007.

[14] M. W. Bloomfield, J. E. Herencia and P. M. Weaver. "Optimization of anisotropic composite plates using an increased design envelope of ply orientations," *Proceedings 49th AIAA/ASCE/ASME/AHS SDM Conference*, Schaumburg, IL, 2008.

[15] M. I. Friswell, J. E. Herencia, D. Baker and P. M. Weaver. "The optimization of hierarchical structures with applications to morphing aircraft," *Proceedings 2nd International Conference on Multidisciplinary Design Optimization and Applications*, 2008. www.asmdo.com/conference2008/

[16] J. E. Herencia, P. M. Weaver and M. I. Friswell. "A fast optimization technique for preliminary sizing of anisotropic composite stiffened panels," *Proceedings 2nd International Conference on Buckling and Postbuckling Behaviour of Composite Laminated Shell Structures*, 2008.

[17] J. E. Herencia, J. E., R. T. Hatfka, P. M. Weaver and M. I. Friswell. "Lay-up optimization of composite stiffened panels using linear approximations in lamination space," *AIAA Journal*, 46:2387–2391, 2008.

[18] J. E. Herencia, P. M. Weaver and M. I. Friswell. "Initial sizing optimization of anisotropic composite panels with T-shaped stiffeners," *Thin-Walled Structures*, 46:399–412, 2008.

[19] H. H. Hilton, D. H. Lee and A. R. A. El Fouly. "General analysis of viscoelastic designer functionally graded auxetic materials engineered/tailored for specific task performances," *Mechanics of Time-Dependent Materials*, 12:151–178, 2008.

[20] H. H. Hilton and S. Yi. "Analytical formulation of optimum material properties for viscoelastic damping," *Journal of Smart Materials and Structures*, 1:113–122, 1992.

[21] C. E. Beldica and H. H. Hilton. "Analytical simulations of optimum anisotropic linear viscoelastic damping properties," *Journal of Reinforced Plastics and Composites*, 18:1658 –1676, 1999.

[22] H. H. Hilton. "Optimum viscoelastic designer materials for minimizing failure probabilities during composite cure," *Journal of Thermal Stresses*, 26:547–557, 2003.

[23] H. H. Hilton. "Designer viscoelastic materials tailored to minimize probabilistic failures for thermal stress induced dynamic column creep buckling," *Journal of Thermal Stresses*, 29:403–421, 2006.

[24] H. H. Hilton. "Optimum viscoelastic material properties tailored to minimize probabilistic failures for thermal stress induced column creep buckling," *Proceedings of the Sixth International Congress on Thermal Stresses* (F. Ziegler, R. Heuer and C. Adam, Eds.), 2:611-614, Technische Universität, Vienna, Austria, 2005.

[25] H. H. Hilton. "Optimum linear and nonlinear viscoelastic designer functionally graded materials – characterization and analysis," *Composites Part A: Applied Science and Manufacturing*, 36:1329–1334, 2005.

[26] H. H. Hilton. "A novel approach to structural analysis: Designer/engineered viscoelastic materials vs. 'off the shelf' property selections," *Journal of Vacuum Technology & Coating*, 10:23–29, 2009.

[27] H. H. Hilton. "Equivalences and contrasts between thermo-elasticity and thermo-viscoelasticity: a comprehensive critique," *Journal of Thermal Stresses*, 34:488–535, 2011. DOI: 10.1080/01495739.2011.564010

[28] J. Lambros, M. H. Santare, H. Li and G. H. Sapna. "A novel technique for the fabrication of laboratory scale model functionally graded materials," *Experimental Mechanics*, 39:184–190, 1999.

[29] J. Lambros, A. Narayanaswamy, M. H. Santare and G. Anlas. "Manufacture and testing of a functionally graded material," *ASME Journal of Engineering Materials and Technology*, 121:488–493, 1999.

[30] J. L. Abanto-Bueno and J. Lambros. "Investigation of a crack growth in functionally graded materials using digital image correlation," *Engineering Fracture Mechanics*, 69:1695–1711, 2002.

[31] J. L. Abanto-Bueno and J. Lambros. "Mechanical and fracture behavior of an artificially ultraviolet-irradiated ploy(ethylene carbon monoxide copolymer," *Journal of Applied Polymer Science*, 92:139–148, 2004.

[32] J. L. Abanto-Bueno. "Fracture of a model functionally graded material manufactured from a photo-sensitive polyethylene," *Ph. D. Thesis in Aerospace Engineering*, University of Illinois at Urbana-Champaign, 2004.

[33] H. H. Hilton and S. T. Ariaratnam. "Invariant anisotropic large deformation deterministic and stochastic combined load failure criteria," *International Journal of Solids and Structures*, 31:3285–3293, 1994.

[34] H. H. Hilton. "Pitching instability of rigid lifting surfaces on viscoelastic supports in subsonic or supersonic potential flow," *Advances in Solid Mechanics*, 1–19, Edwards Bros., Ann Arbor, 1957.

[35] H. H. Hilton. "The divergence of supersonic, linear viscoelastic lifting surfaces, including chord-wise bending," *Journal of the Aero/Space Sciences*, 27:926–934, 1960.

[36] H. H. Hilton and C. F. Vail. "Bending-torsion flutter of linear viscoelastic wings including structural damping," *Proceedings AIAA/ ASME/ASCE/ AHS/ASC 33rd Structures, Structural Dynamics and Materials Conference, AIAA Paper 93-1475*, 3:1461–1481, 1993.

[37] C. E. Beldica, H. H. Hilton and S. Yi. "A sensitivity study of viscoelastic, structural and piezoelectric damping for flutter control," *Proceedings 39th AIAA/ASME/ASCE/AHS/ASC Structures, Structural Dynamics and Materials Conference, AIAA Paper 98-1848*, 2:1304–1314, 1998.

[38] C. E. Beldica, H. H. Hilton and D. Kubir. "Viscoelastic panel flutter - stability, probability of failure and survival times," *Proceedings of the 42nd AIAA/ASME/ ASCE/AHS/ASC Structures, Structural Dynamics and Materials Conference, AIAA Paper 2001-1647*, 5:3423–3433, 2001.

[39] H. H. Hilton and C. E. Beldica. "Nonlinear viscoelastic damping, piezoelectric control and probability of failure of light weight plates subjected to aerodynamic noise," *Proceedings of the Seventh AIAA/ CEAS Aeroacoustics Conference, AIAA Paper 2001-2233*, 2:736–746, **CD-ROM Vol.**, Maastricht, the Netherlands, 2001.

[40] H. H. Hilton. "An introduction to viscoelastic analysis," *Engineering Design for Plastics* (E. Baer, ed.), 199–276, Reinhold Publishing Corp., New York, 1964.

[41] H. H. Hilton and S. B. Dong. "An analogy for anisotropic, nonhomogeneous, linear viscoelasticity including thermal stresses," *Development in Mechanics*, 58–73, Pergamon Press, New York, 1964.

[42] R. M. Christensen. *Theory of Viscoelasticity - An Introduction, 2nd ed.* Academic Press, New York, 1981.

[43] H. H. Hilton. "On the inadmissibility of separation of variables solutions in linear anisotropic viscoelasticity," *International Journal of Mechanics of Composite Materials and Structures*, 3:97–100, 1966.

[44] L. C. Brinson and T. S. Gates. "Effects of physical aging on long term creep behavior of polymers and polymer matrix composites," *NASA TM 109081, 1994. International Journal of Solids and Structures*, 32:827–846, 1995.

[45] M. E. Tuttle and H. F. Brinson. "Accelerated viscoelastic characterization of T300/5208 graphite-epoxy laminates," *NASA Contractor Report 3871*, Washington, 1985.

[46] M. R. Monaghan, L. C. Brinson and R. D. Bradshaw. "Analysis of variable stress history on polymeric composite materials with physical aging," *Composites Engineering*, 4:1023–1032, 1994.

[47] M. R. Monaghan and L. C. Brinson. "Analysis of variable stress history on polymeric composite materials with physical aging,“ *Proceedings of International Conference on Composites Engineering/1* (D. Hui, ed.), 69-70, 1994.

[48] G. C. F. M. R. Baron de Prony. "Essai experimental et analytique," *Journal de l'École Polytechnique de Paris*, 1:24–76, 1795.

[49] C. A. de Coulomb. *Théorie des machines simples, en ayant égard au frottement de leurs parties et à la roideur des cordages*, Bachelier, Paris, 1821

[50] R. L. Bisplinhoff and H. Ashley. *Principles of Aeroelasticity.* John Wiley & Sons, New York, 1962.

[51] L. Euler. "Additamentum I de curvis elasticis, methodus inveniendi lineas curvas maximi minimivi proprietate gaundentes," *Opera Omnia I*, 24:23–297, 1744.

[52] H. H. Hilton. "Creep collapse of viscoelastic columns with initial curvatures," *Journal of the Aeronautical Sciences*, 19:844–846, 1952.

[53] C. Libove. "Creep buckling of columns," *Journal of the Aeronautical Sciences*, 19:459–467, 1952.

[54] H. H. Hilton. "On the nonexistence of finite critical times for generalized linear viscoelastic columns with arbitrary initial curvatures," *Journal of the Aero/Space Sciences*, 28:655–656, 1961.

[55] J. Kempner and F. V. Pohle. "On the non-existence of a finite critical time for linear viscoelastic columns," *Journal of the Aeronautical Sciences*, 20:572–573, 1953.

[56] A. D. Drozdov and V. B. Kolmanovskii. *Stability in Viscoelasticity,* Elsevier, Amsterdam, 1994.

[57] N. J. Hoff, B. A. Boley and J. A. Coan. "The development of a technique for testing stiff panels in edgewise compression," *Proceedings of the Society for Experimental Stress Analysis*, 5:14–24, 1948.

[58] J. Singer, J. Arbosz and T. Weller. *Buckling Experiments: Experimental Methods in Buckling of Thin-Walled Structures – Basic Concepts, Columns, Beams and Plates*, Vol.1, John Wiley & Sons, New York, 1998.

[59] R. M. Jones. *Buckling of Bars, Plates, and Shells*, Bull Ridge Publishing, Blacksburg, VA, 2006.

[60] H. H. Hilton. "Viscoelastic column dynamic creep buckling– failure probabilities and survival times," *Proceedings International Conference on Nonlinear Problems in Aviation and Aerospace*, 18, Melbourne, FL, 2002.

[61] H. H. Hilton. "Linear viscoelastic dynamic torsional divergence of wings and creep buckling of columns including failure probabilities and survival times," submitted to *Journal of Aeroelasticity and Structural Dynamics*, 2011.

[62] G. Gerard. *Introduction to Structural Stability Theory,* McGraw-Hill, New York, 1962.

[63] F. R. Steinbacker and G. Gerard. *Aircraft Structural Mechanics,* Pitman Publishing Co., New York, 1952.

[64] F. R. Shanley and E. I. Ryder. "Stress Ratios: The Answer to the Combined Loading Problem," *Aviation*, 36:28–29, 43, 66, 69–70, 1937.

[65] J. M. Lifshitz and A. Rotem. "Time-dependent longitudinal strength of unidirectional fibrous composites," *Fibre Science and Technology*, 3:1–20, 1970.

[66] S. L. Phoenix. "Statistical aspects of failure of fibrous materials," *Composite Materials: Testing and Design, ASTM STP 674*, (S. W. Tsai, Ed.), 455–483, 1979.

[67] S. L. Phoenix and L-J. Tierney. "A statistical model for the time dependent failure of unidirectional composite materials under local elastic load-sharing among fibers," *Engineering Fracture Mechanics.* 8:193–215, 1982.

[68] D, A. Dillard and H. L. Brinson. "A numerical procedure for predicting creep and delayed failures in laminated composites," *Long-Term Behavior of Composites, ASTM STP 813*, T. K. O'Brien, (ed.), 23–37. ASTM, Philadelphia, 1983.

[69] C. Hiel, M. Sumich and D. P. Chappell. "A curved beam test specimen for determining the interlaminar tensile strength of a laminated composite," *Journal of Composite Materials*, 25:854–868, 1991.

[70] A. S. Watson and R. L. Smith. "An examination of statistical theories for fibrous materials in the light of experimental data," *Journal of Materials Science*, 20:3260–3270, 1985.

[71] H. H. Hilton and S. Yi. "Stochastic viscoelastic delamination onset failure analysis of composites," *Journal of Composite Materials*, 27:1097–1113, 1994.

[72] W. Weibull. "A statistical distribution function of wide applicability," *ASME Journal of Applied Mechanics*, 18:293–297, 1951.

[73] E. S. Lindquist. "Strength of materials and the Weibull distribution," *Journal of Probabilistic Engineering Mechanics*, 9:191–194, 1994.

[74] D. Murthy, N. Prabhakar, M. Xie and R. Jiang. *Weibull Models.* John Wiley & Sons, Hoboken, 2004.

[75] N. J. Hoff. *The Analysis of Structures,* John Wiley & Sons, New York, 1956.

[76] E. Isaacson and H. B. Keller. *Analysis of Numerical Methods.* Dover Publications, New York, 1966.

[77] A. R. Zak. "Structural analysis of realistic solid propellant materials," *Journal of Spacecraft and Rockets*, 5:270–275, 1967.

[78] R. L. Taylor, K. L. Pister and G. L. Goudreau. "Thermomechanical analysis of viscoelastic solids," *International Journal for Numerical Methods in Engineering*, 2:45–59, 1970.

[79] S. Yi, G. D. Pollock, H. H. Hilton and M. F. Ahmad. "Time dependent analysis of anisotropic viscoelastic composite shell structures," *International Journal of Computing Systems in Engineering*, 3:457–467, 1992.

[80] S. Yi and H. H. Hilton. "Hygrothermal effects on viscoelastic responses of laminated composites," *International Journal of Composites Engineering*, 5:183–193, 1995.

[81] S. Yi, M. F. Ahmad and H. H. Hilton. "Dynamic responses of plates with viscoelastic damping treatment," *ASME Journal of Vibration and Acoustics*, 118:362–374, 1996.

[82] S. Yi, S. F. Ling, M. Ying, H. H. Hilton and J. R. Vinson. "Finite element formulation for anisotropic coupled piezo-hygro-thermo-viscoelastodynamic problems," *International Journal of Numerical Methods in Engineering*, 45:1531–1546, 1999.

[83] H. H. Hilton and S. Yi. "Stochastic viscoelastic delamination onset failure analysis of composites," *International Journal of Composite Materials*, 27:1097–1113, 1993.

[84] S. Yi and H. H. Hilton. "Dynamic finite element analysis of viscoelastic composite plates in the time domain," *International Journal for Numerical Methods in Engineering*, 37:4081–4096, 1994.

[85] H. H. Hilton and S. Yi. "Anisotropic viscoelastic finite element analysis of mechanically and hygrothermally loaded composites," *International Journal of Composites Engineering*, 3:123–135, 1992.

[86] H. H. Hilton and H. G. Russell. "An extension of Alfrey's analogy to thermal stress problems in temperature-dependent linear viscoelastic media," *Journal of Mechanics and Physics of Solids*, 9:152–164, 1961.

[87] H. H. Hilton and J. R. Clements. "Formulation and evaluation of approximate analogies for temperature-dependent linear viscoelastic media," *Thermal Loading and Creep*, Institution of Mechanical Engineers, London, UK, 6-17 to 6-24, 1964.

[88] E. H. Dowell. *Aeroelasticity of Plates and Shells,* Noordhoff International Publishers, Leiden, 1975.

[89] E. Dowell and M. Ilgamov. *Studies in Nonlinear Aeroelasticity.* Spring-Verlag, New York, 1988.

[90] E. H. Dowell, R. Clark, D.Cox, H. C. Curtis Jr., J. W. Edwards, K. C. Hall, D. A. Peters, R. H. Scanlan, E. Simiu, F. Sisto and T. W. Starganac. *A Modern Course in Aeroelasticity.* Kluwer Academic Publishers, Boston, 2004.

[91] H. H. Hilton and J. J. Piechocki. "Shear center motion in beams with temperature dependent linear elastic or viscoelastic properties," *Proceedings Fourth United States National Congress of Applied Mechanics* 2:1279–1289, ASME, 1962.

[92] C. G. Merrett and H. H. Hilton. "Influences of starting transients, aerodynamic definitions and boundary conditions on elastic and viscoelastic wing and panel flutter," *Journal of Mathematics, Engineering, Science and Aerospace*, 2:121–144, 2011.

[93] P. H. Geubelle, M. J. Danyluk and H. H. Hilton. "Dynamic mode III fracture in viscoelastic media," *International Journal of Solids and Structures*, 35:761–782, 1997.

[94] M. J. Danyluk, P. H. Geubelle and H. H. Hilton. "2D and 3D dynamic fracture in viscoelastic materials," *International Journal of Solids and Structures*, 35:3831–3853, 1998.

[95] M. J. Lighthill. "On sound generated aerodynamically. I. General theory," *Proceedings of the Royal Society (London)*, 222A:564–587, 1952.

[96] M. J. Lighthill. "On sound generated aerodynamically. II. Turbulence as a source of sound," *Proceedings of the Royal Society (London)*, 231A:1–32, 1954.

[97] M. E. Goldstein. *Aeroacoustics*, McGraw-Hill, New York, 1976.

[98] W. R. Sears. "Some aspects of non-stationary airfoil theory and its practical applications," *Journal of the Aeronautical Sciences*, 8:104–108, 1941.

[99] M. Abramowitz and I. A. Stegun, Eds. *Handbook of Mathematical Functions.* National Bureau of Standards, Washington, DC, 1964.